Attainable Artificial Gravity And Space Radiation Protection Solutions For Interplanetary Spaceships

by
Timothy Kyle Bishop

A thesis submitted to the Mechanical Engineering Department,
Cullen College of Engineering
in partial fulfillment of the requirements for the degree of

MASTER OF SCIENCES

in Space Architecture

Chair of Committee: Olga Bannova

Committee Member: Larry Bell

Committee Member: Kriss Kennedy

Committee Member: Larry Toups

University of Houston
May 2020

DEDICATION/EPIGRAPH

To Frank and Mahlon Weber, in memory

To Bill and Jan Bishop

To my lovely Wife, Nicole

To my family, Mum Yun Ja, Dad Robert and Sister Natasha

To God, who walks with me

ACKNOWLEDGMENTS

I would like to acknowledge the SICSA faculty, thank you to Professor Olga Bannova for the discussions and encouragement over the years. Your patience during my journey at SICSA has been much appreciated and I truly appreciate the guidance and assistance as I've struggled to find my path within the space architecture community.

Thank you to Kriss Kennedy for the tremendous guidance and knowledge you have imparted on me. You have shown me alternative avenues of thinking and I've enjoyed your classes very much.

Thank you to Larry Bell for the insightful discussions we have had. You have pulled me out of the enormous scope creep I was experiencing and I'm glad we got the chance to have our discussions on space architecture and artificial gravity.

Thank you to Larry Toups for the constant gestures of support and out-of-the-box thinking. You have exposed me to ideas that have been thought provoking, and have introduced me to professionals in the industry I would not have otherwise met.

I would also like to acknowledge my fellow classmates for the enlightening discussions and late nights discussing the intricacies of space dynamics: Zach Taylor, Taylor Phillips-Hungerford, Brett Montoya, Thomas Lagarde and Albert Rajkumar.

ABSTRACT

Spacecraft habitats designed for long duration human spaceflight currently lack feasible designs to protect the crew from the harmful effects of micro-gravity and space radiation. Prolonged exposure to micro-gravity can lead to various health issues while space radiation exposure varies from long-term illness to acute radiation poisoning with possible fatal doses. This thesis explores these issues in order to derive a design solution for a spacecraft habitat capable of protecting the crew from both micro-gravity effects and space radiation exposure.

Radiation simulations were performed to gather data on the stopping power of spacecraft hulls when exposed to galactic cosmic radiation and solar particle events. The hulls were augmented with various materials of varying thicknesses to ascertain how effective and feasible it would be to construct a spacecraft out of traditional construction methods, while adding a radiation protection layer. An analysis into artificial gravity habitat topology was conducted to determine feasibility in design sizes and geometries. A torus shape was determined to be the optimal topology.

An emphasis was placed on the concepts of operations of the spacecraft habitat construction as well as the interior structural assembly. The spacecraft habitat utilizes a combination of hard-shell modules and curved inflatable modules to form an idealized geometry suitable for spacecraft rotation, for the purposes of generating artificial gravity. The interior of the spacecraft was outfitted with sub-systems, equipment and furniture to visualize the habitat in a way that communicates the potential of the design.

TABLE OF CONTENTS

LIST OF TABLES

LIST OF FIGURES

I INTRODUCTION

Humanity is on the brink of embarking on the next chapter of civilization, travelling to other planets in our solar system. Numerous government agencies and private companies have announced plans to build spaceships to take us there while also establishing permanent settlements on the Moon and Mars. Much work is still required for humanity to write this next chapter, and we will need spaceships that are specific to suit our own needs for surviving deep space. Humanity must do all it can do ensure the success of the first voyages to other planets or face public retaliation and abandonment of the human space fairing dream, potentially postponing writing that next chapter.

This thesis study proposes an approach and concepts for the design and construction of future spaceship habitats, that provide the necessary technologies to ensure the success of human voyages into deep space, with the following vision:

"To build a fleet of versatile spacecraft, sending humans anywhere within the solar system, and beyond."

It is the mission of this author to provide a sound and feasible methodology for the construction of a spacecraft habitat providing realistic solutions to bridge two large technology gaps as outlined by the National Aeronautics and Space Administration (NASA) Human Research Program (HRP). The first involves the integration of artificial gravity technology systems. The application of such systems allows a crew to experience a centripetal force on their entire body, serving to minimize the damaging of effects of micro-gravity on humans, such as bone loss, vision impairment and muscle atrophy. The second adds space radiation countermeasures to the spacecraft to protect both the human crew and sensitive equipment from hazardous doses. Neither technology has achieved a technology readiness level (TRL) of

9 (National Aeronautics and Space Administration (NASA), 2017), which defines technologies in this category as flight proven technologies through successful mission operations.

The first goal of this thesis designs a spacecraft habitat capable of supporting extended human missions to other celestial bodies. Key objectives are to ensure the habitat is capable of supporting humans for a total of five years, to provide realistic methods of construction and maintenance and to provide avenues of component upgrade and replacement.

The second goal integrates a feasible artificial gravity system capable of construction utilizing current or near-term launch vehicle capabilities. The key objectives are to ensure the feasibility of such a system by designing to meet the minimum requirements for crew, to account for the systems construction, and to minimize system complexity.

The final goal incorporates a feasible space radiation countermeasure concept which is quantitively validated to protect the crew. The objectives are to present a passive solution, requiring zero powered sub-system support, to meet the NASA maximum recommended annual radiation dosage limits and to protect from the worst-case scenario's regarding solar proton storms.

This thesis addresses an attainable combination of solutions to construct a deep-space spacecraft habitat for humans employing current and emerging technologies that generate artificial gravity for the crew, while also providing sufficient protection from space radiation. The primary goal of this thesis study is to add value to the human spaceflight community's data, planning and designs for future human missions to the Moon, Mars and further into deep space.

II SPACECRAFT REQUIREMENTS

A review of the literature for spacecraft integrated with artificial gravity systems was undertaken. Furthermore, a review of the space radiation environment was conducted to understand the optional radiation protection issues and countermeasures to identify and assess which materials are most applicable. Summary requirements and conclusions derived from the review are applied to drive the spacecraft habitat design.

II.1 Literature Review

Spacecraft and habitat design concepts were reviewed that emphasized the need to integrate an artificial gravity system. Within the design proposals identified, the author observed an absence of emphasis regarding the internal habitat layouts of spacecraft, with regards to integrated artificial gravity systems. This review is specific to the habitat design of a rotating spacecraft, the overall physical spacecraft design and the integration of humans into an artificial gravity system.

A review of the literature pertaining to space radiation protection measures was conducted to determine the composition of the space radiation environment and the health effects the space radiation environment have on the crew. With an emphasis on passive radiation protection, materials were reviewed for their radiation protection value relative to the lethality of risks and countermeasures for exposed crew members. The review first investigated space radiation composition in the general environment, followed by the health effects associated with exposure to the environment. It finally examines which passive measures can be utilized to protect from the environment to prevent illness.

II.1.1 Spacecraft Artificial Gravity

The internal topology of a habitat that employs an artificial gravity system can come in many different forms. There exists a trade space between the habitat's radius, the spin rate

and the level of comfort of the crew. Figure 1 identifies the trade space of habitat topologies for artificial gravity habitats:

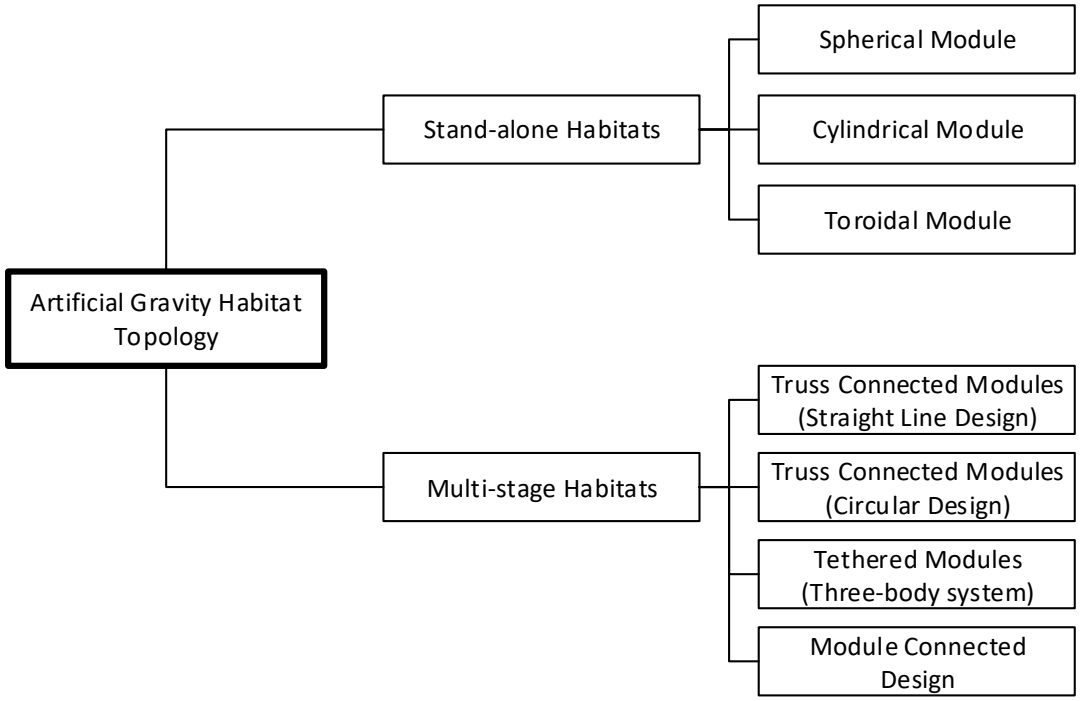

Figure 1: Habitat Trade Tree for Artificial Gravity

Stand-alone habitats refer to habitats that are packed and deployed in a single launch. These modules could be hard shell modules, such as those used for the International Space Station (ISS); or they could be inflatable modules and expand beyond the limitations of the payload fairing radius they were launched in. These modules would utilize the interior radius of their structure as the platform on which the crew would stand when subjected to centrifugal forces. According to a review by Hall, the literature has set an upper limit to the spin rate at 6 revolutions per minute (RPM), and a minimum tangential velocity of 6 meters per second (m/s) (Hall, Artificial Gravity in Theory and Practice, 2016). Applying centripetal force calculations derived, the minimum radius is 10 meters (20m dia) (Hall, SpinCalc, 2018). Current launch vehicles have payload fairing diameters of approximately 5 meters (m), inflatable modules would need to expand by a factor of four to achieve the minimum size

requirements. As of this writing, the space industry has not recognized an inflatable habitat configuration with a diameter extending to 20 m. The closest known habitat is the Bigelow Olympus module, with a design diameter of 12.6 m (Bigelow Aerospace, 2011). The use of inflatables plays an important role, as this technology allows for the packing of larger habitats into conventional payload fairings, such as Bigelow's habitats.

Centripetal force levels, i.e. gravity levels (g-levels) are compared to radii, increasing the radius allows for the decrease of the rotation rate, while preserving the g-level. Decreasing the rotation rate affords the crew ever-increasing levels of comfort; however, comfort level testing in a space environment has yet to be performed since the analysis is dependent on real-world data. Utilizing a cylinder or spherical inflatable with an internal rotating track is possible however, this method is solely dependent on the internal maximum radius of the habitat and is therefore identified as an upper limit for this type of design. Upon an examination of the Bigelow B330, the radius would not facilitate much sufficient g-levels due to the small radius (Bigelow Aerospace, 2018).

The Near-Term Artificial gravity concepts for deep space missions AIAA – SciTech 2019 paper describes single module habitats for Artificial Gravity. It is a comprehensive review of the current state of the art for artificial gravity technologies. Much emphasis was placed on rotating surfaces inside large cylindrical tanks, with a focus on reusing tanks for habitats. (Zipay, 2019). However, the internal radius is limited to the launch vehicle payload fairing radius which is currently set a 5 m limit (assuming the SLS Block 1B). This is not large enough according to Hall in his paper Artificial Gravity in Theory and Practice where his review indicates that a minimum radius of 12 m is required to fulfil the crew comfort level limits (Hall, Artificial Gravity in Theory and Practice, 2016).

Figure 2: Concept utilizing large SLS tank for artificial gravity (Zipay, 2019)

Multi-module habitats refer to numerous modules assembled to form a habitat that is suitable for the rotating motion required for artificial gravity. Truss connected modules in a straight line, as shown in Figure 3 demonstrates connecting two habitat modules, or a habitat module with a counter-weight together configuration for a rotating spacecraft. The spacecraft rotates about the center of mass (green arrows indicate rotation). Jevtovic's work provides an example of this configuration (Jevtovic, 2015). For a double habitat design, crew isolation becomes a potential issue, since keeping the crew separated during long duration missions introduces unknown psychological effects the literature currently has no data on. A solution is to provide a method to connect the two modules together allowing the crew to transfer from one module to another. This configuration also creates another problem where the center of mass is constantly shifting due to the constant crew movement, introducing instabilities into the spacecraft's rotation.

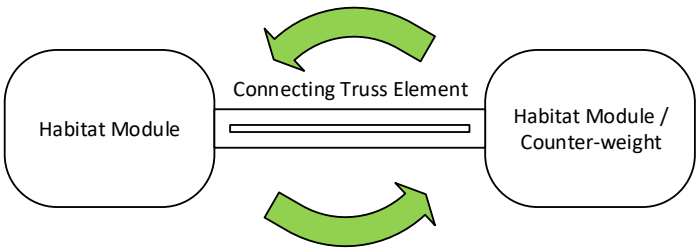

Figure 3: Truss Connected Module

The study by Joosten and their team provides an understanding of the design requirements and the interfaces required to design a feasible artificial gravity spacecraft. The study focused on spacecraft mass penalties and mission performance, with designing to constraining the artificial gravity to 1g at 4 rpm, shown in Figure 4. A Mars mission was assumed with an artificial gravity system integration as the primary requirement. This approach utilizes the spacecrafts systems to counterbalance each other and maintain a center of mass near the center of the spacecraft where the propellant tanks are located.

The construction approach utilizes an extendable coilable mast truss structure with a habitation module at one end, power systems at the other end, with propulsion elements at the center. Furthermore, the spacecraft controls the rotational spin using propulsion system elements to de-spin the spacecraft that allow thrust vectoring without requiring the precession of the angular momentum associated with the rotating sections (Joosten, 2007). The design allows for a slow rotating spacecraft that also keeps the crew at safe distances from the nuclear reactor. The habitat itself provided rigid flooring supported by cables and emulated a gravity environment.

The habitat design is limited to a single inflatable module which presents a single fault tolerant situation should the habitat experience a rapid depressurization. The habitat layout does not seem to account for Coriolis forces (Hall, Artificial Gravity in Theory and Practice, 2016). The rotation must be de-spun for other spacecraft to dock with the habitat and there appears to be a single point of ingress/egress. Assembly concept of operations has not been explored; however, this critique is mentioned.

Joosten's work provides a solution to the course correction problem by utilizing low thrust vectoring during rotation. The assumption of the incorporation of low thrust thrusters into the thesis design philosophy will likely influence the layout of the habitat. The use of

inflatables to increase the internal volume while maintaining a smaller launch payload profile is useful given the diameter constraints of launch vehicles. Integrating inflatable habitat architectures will contribute to the feasibility of the thesis design.

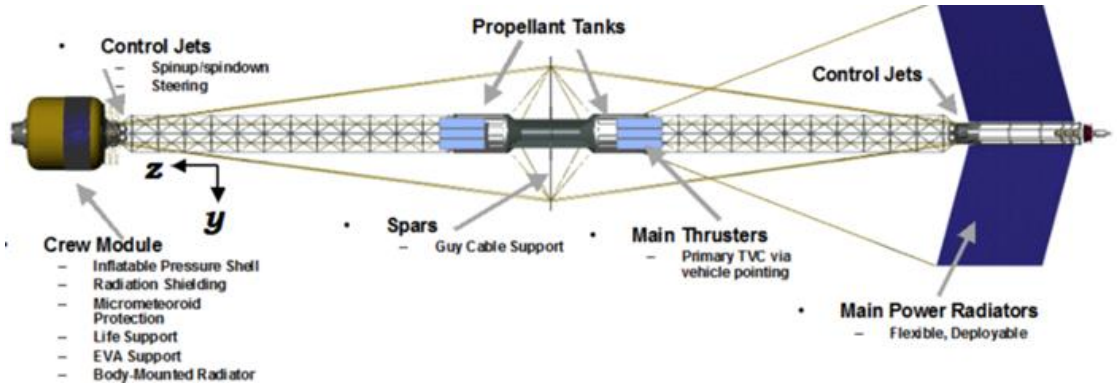

Figure 4: Joosten Spacecraft Design

Truss connected modules in a circular form are represented in Figure 5 and take advantage of adhering to the radius that is affected by the artificial gravity gradients. This configuration avoids the seemingly unusable volume (for artificial gravity purposes), since this volume would be subjected to less centrifugal forces than at the radius. The crew would have the same isolation issues as the previous design, however if the modules were connected to allow for crew movement and transfer then this again would solve this problem. The issue still remains for the mass distribution affecting the center of mass, but since the design is circular, the distribution is spread more evenly along the entire radius, thus having less impact.

A connected module topology shown in Figure 5, demonstrates habitat modules to be built radially outward from a center module. The connected topology allows for the crew to move freely about the habitat unimpeded by separated modules. During habitat rotation, the crew is subjected to the largest centripetal forces at the ends of the modules and the least amount of centripetal forces at the center. Traversing through this habitat while rotating would also subject the crew to Coriolis forces, which is discussed in section III.2.1. The topology

requires optimization to ensure the crew allocate the majority of their time at a certain radius of the habitat to maximize time at the largest g-levels possible.

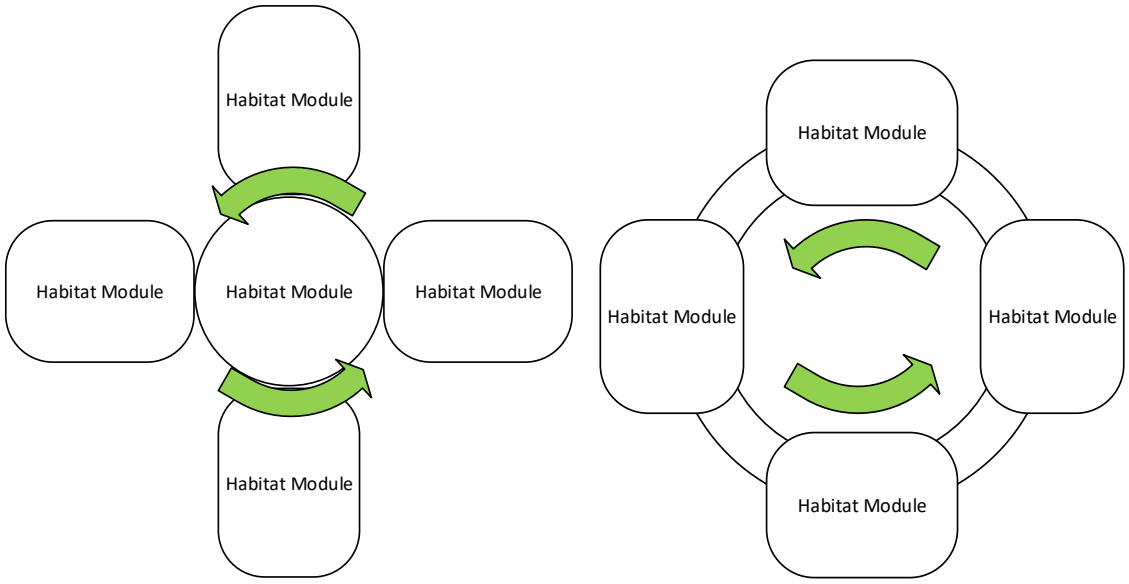

Figure 5: Connected Module (left) and Circular Module (right) Topology

The Nautilus-X spacecraft (Holderman, 2011) (Henderson & Holderman, 2011) concept is an exo-atmospheric spacecraft concept with multi-mission capabilities and addresses the need for an artificial gravity system for deep space spacecraft. It was developed by the by the NASA Technology Application Assessment Team. The spacecraft was estimated to utilized 2-3 High-mass Launch Vehicles (HLV) plus additional crew vehicles in its construction, maintain a crew of six for two years and a 64-month construction duration.

The integration of the artificial gravity system provides artificial gravity to the crew utilizing soft wall inflatables supported by stabilization rings and trusses, and an independent low thrust propulsion system. The artificial gravity system rotates independent of the rest of the spacecraft, allowing for continuous docking operations without the need to de-spin. The Nautilus-X incorporates a unique interchangeable propulsion element design, which requires the propulsion element be mission specific. The advantage to this design decision is the large

mass savings that come with utilizing only what fuel tanks and thrusters are necessary per the mission planned.

The artificial gravity system will introduce conservation of momentum effects to the rest of the spacecraft, meaning the spacecraft will rotate counter to the rotation of the artificial gravity system in order to conserve angular momentum. This may have unintended consequences on navigation and docking. The artificial gravity system is integrated with a dynamic ring flywheel, it is unclear how the two structures maintain an effective pressure seal since pressure seals in space habitats are known to leak. This is one reason why the ISS requires frequent supplies of additional nitrogen and oxygen tanks. It is understood rotating seals do not perform as well as static pressure seals. The crew will continuously be required to traverse from the artificial gravity system to other parts of the spacecraft, this could increase the adjustment time to both rotating and static reference frame and may in fact hinder crew performance due to the inability of the crew to fully adjust. This claim is unproven until tests for rotating habitats are performed in the space environment.

The design approach for an integrated propulsion system is worth exploring in the thesis design. The use of soft wall inflatables provides validation that feasible solutions exist to construct large ring like structures for artificial gravity systems. The Nautilus-X is a solid premise for this thesis with the design philosophy that supports the feasibility of constructing a multi-mission exploration spacecraft.

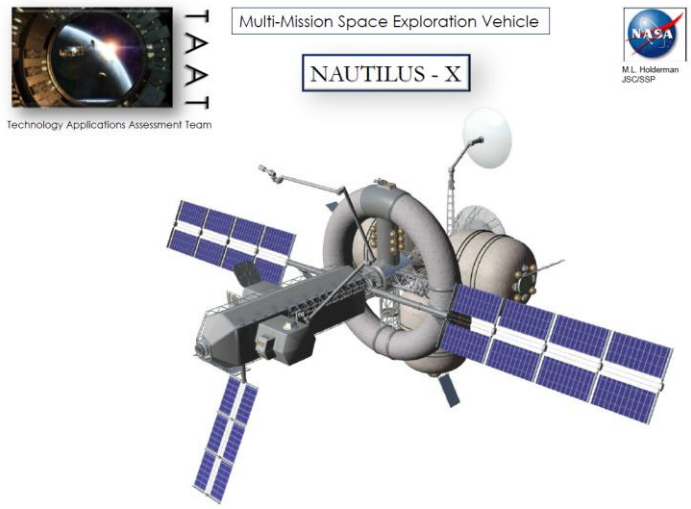

Figure 6: NAUTILUS-X MMSEV Concept

The Electrodynamic Gravity Generator (Jevtovic, 2015) utilizes superconducting magnetics to create a rotary motor that allows for an electrically powered gravity system. The paper outlines utilizing technology currently applied in maglev trains and wind turbine generators, highlighting the technology maturity and the lower technology barriers for integrating into a space environment. Jevtovic did specify that the motors are solar powered and are to be utilized for deep space operations.

Electrically powered systems eliminate the thruster requirement which removes the need for its supporting systems such as fuel and structure assemblies. The design allows for dual rotating assemblies to spin counter to one another, removing the conservation of momentum artifact mentioned earlier in the Nautilus-X critique. The design is also scalable and reconfigurable since the rotating motors are located at the central axis of the design, allowing for multiple habitat configurations to exist. Figure 7 shows an asymmetric configuration with a "wheel" of habitats connected to a dual-arm habitat structure.

The design will likely require cooling systems since the superconductors are in close proximity to the pressurized habitat, and the heat transfer from the modules will transfer to the superconductor motors. A cooling system is necessary since superconductors require

extreme cold temperatures to operate, this presents unique thermal challenges. As discussed with the Nautilus-X, rotating seals are likely required for atmospheric pressurization. Incorporating dual rotating seal systems will likely increase the rate of atmospheric leakage.

An electrically powered rotation system for the deployment of artificial gravity systems is something worth exploring in this thesis as it may present new methods for generating the required g-level conditions. The reconfigurable approach to spacecraft design supports the need for a spacecraft to remain flexible, if it is to be applicable to the largest scope of missions possible.

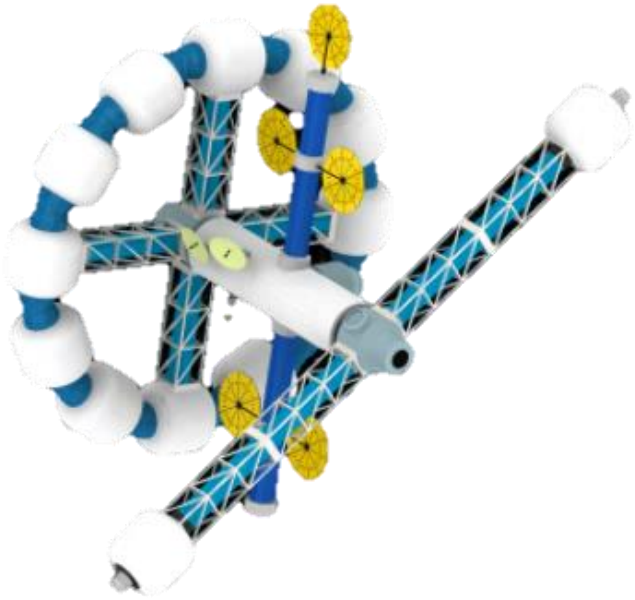

Figure 7: Jevtovic Spacecraft Design

The Hyperion spacecraft was designed to provide artificial gravity for a Mars bound crew while utilizing an ion propulsion system. Emphasis was placed on propellant reduction and artificial gravity, utilizing aerobraking techniques to reduce the propellant cost and integrating a counterweight to the habitation module (Minster, et al., 2018).

The design utilizes a unique curved habitat design that functions to maintain the crew at an equal distance from the center of rotation as they walk about the habitat, shown in Figure 8. The design team chose to rotate the spacecraft at 3.3 RPM with a rotational radius of 30.9 m, providing the crew with Mars like g-levels (0.38 g). The spacecraft includes expandable truss elements for the structure, allowing for in-space construction employing current generation launch vehicles. Ion thrusters and gimbals provide rotation and attitude control as well as efficient fuel usage. The use of ion thrusters further promotes their use in the functional architecture for the thesis design.

Although detail of the habitat layout is not within the scope of this design, habitat volume was a primary metric in determining habitat size. A key feature of the Hyperion design is the curved toroid section utilized for its habitat as it ensures the crew maintain a constant distance from the rotation axis. A curved surface is beneficial to the crew; however, it is unclear how it would be manufactured. Furthermore, the curved geometry may introduce increased pressure at certain places in the habitat at the cabin pressure will try to equalize at all points. Additional structure might be required to accommodate for the pressure differences. It was discussed the curved geometry of the habitat had an arclength of 17 m(Minster, et al., 2018), yet surface area within the habitat was not discussed. For an artificial gravity environment, surface area might be an important metric to track even more than volume. As with Joosten's design, the Hyperion spacecraft requires a de-spin operation to allow another spacecraft to dock with it. Nevertheless, a curved surface for the crew appears to be quite beneficial and incorporating such a design concept for this thesis may prove to be worthwhile.

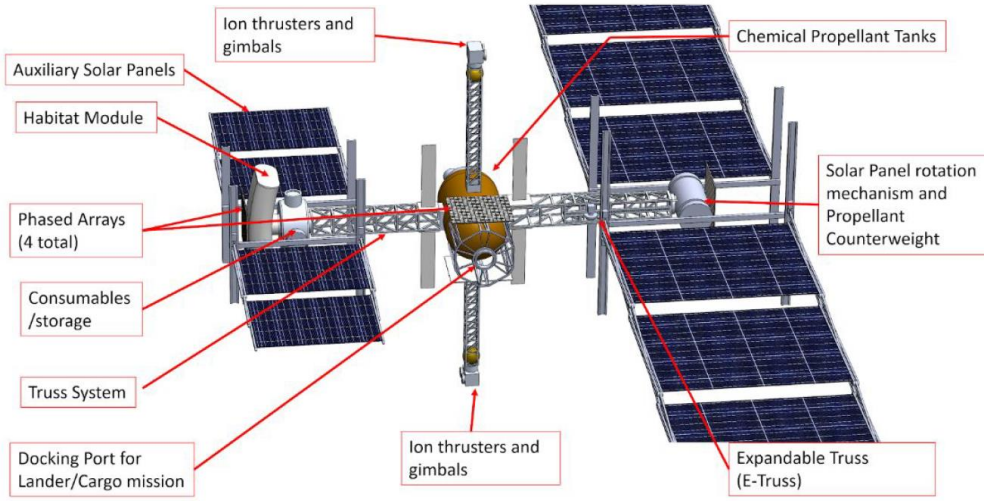

Figure 8: Hyperion Spacecraft Design

II.1.2 Space Radiation

Space radiation is comprised of GCR and SPE, each have different sources and interact with the human body in unique ways. A review of the SPE data from 1997-2006 by Cane, Richardson, & von Rosenvinge, (2010) revealed higher concentrations of H and He ions in the SPE composition but with lower energies when compared with the energies of these ions present in GCR. The data showed energies of H/He at ~67 MeV and O/Fe at ~34 MeV, these were analyzed due to their significance. In comparison, proton specific GCR kinetic energies tend to peak in the ~200 MeV range (Boezio & Mocchiutti, 2012) based on data from 2006-2009 PAMELA mission.

A review of the composition ratio between H/He ion and O/Fe ions reveal the ratio's can vary up to factor of 10,000 (Cane, Richardson, & von Rosenvinge, 2010), with there being vastly higher concentratinos of H/He in the SPE composition. This suggests that the primary elements SPE are composed of are H/He ions. GCR has been recorded to have 85% H, 14% He, 1% all other elements (Durante & Cucinotta, 2011). Mrigakshi, Matthia, Berger, Reitz, & Wimmer-Schweingruber, (2013) references Simpson's (1983) GCR composition with slightly

different values for H/He composition with 87% H and 12% He. This difference does not affect the dosage greatly since Wu, et al., (2019) cited C. La Tessa, et al., (2005), discussing about 14% of the dosage from GCR is related to the ~1% heavy elements, with Fe ions contributing the most to this . The radiation dosage is one of the most used metrics for determining how the radiation affects the human body.

There is much research that studies the effects of space radiation's harmful effects on the human body. The mean lethal dose is a measured in the unit gray (Gy) where 2.5 Gy delivered to the human body is the mean lethal dose; furthermore the amount of dosage a SPE can deliver is up to 3.0 Gy. Other side effects besides cancer are cataracts, retinal flashes (experienced by the Apollo crew) and bone marrow issues. (Todd, 2003).

There is a great deal of uncertainty on the associated immediate risk with space radiation exposure, especially when derviving a metric to estimate how much exposure a mission will increase the probability of developing symptoms. The long-term effects are less known than the short term effects, which poses issues for long-duration spaceflight. Unknown risks are either ignored for the sake of costs or create funding issues for the programs. Gaps in knowledge include biological effectiveness of slow developing radiation effects for cancer/non-cancer, errors in dosimetry data, high/low LET exposure and the shape of the low dose dosimetry curve for charged particles (Durante & Cucinotta, 2011). In order to protect from these health effects, whether or not they are known requires protective measures that work to sheild the crew at least in part, to the space radiation environment.

II.1.3 Passive Radiation Shielding

Passive radiation shielding refers to radiation protection methods that do not involve an active system to continuously provide radiation protection. Passive protection typically consist of various materials to slow or stop the particle transport of high energy ions. This

final section of the review discusses the research into passive radiation shielding and seeks to uncover which materials are best suited for the task as well as determining possible configurations to begin the optimization process. Polyethylene is a staple among the literature as a primary method to protect from both GCR and SPE.

Kaul, Barghouty, & Danche, (2004) meausred the effectiveness of polyethylene fiber composite against a 500 MeV/n Fe beam, with polyethylene thicknesses between 1 – 5 cm thick. The high hydrogen content polymers such as polyethylene form excellent shielding when incorporated into a martix resin; furthermore the addtion of boron to the matrix resin further increases the shielding effectiveness by increasing the ability to slow thermal neutrons produced from the GCR/SPE interations (Kaul, Barghouty, & Danche, 2004).

Wu, et al., (2019) performed computational studies on the absorbed dosage of polyethylene, water, carbon fiber and aluminum to measure the effect on a tissue simulant, against an Fe ion beam. The results indicated the depth of the bragg peaks in the tissue simulant decreased as the material thickness increased, implying the highest dosage was occuring at shallower depths inside the tissue simulant as the material thickness increased. Interestingly the gap in aluminum's poor performance continued to increase as the material thicknesses increased, suggesting aluminum should be no more than a few cm's thick to minimize dosage. (Wu, et al., 2019)

Kevlar was evaluated alongside polyethylene in the space environment and produced similar results from a radiation protection performance perspective. The European Space Agency (ESA) funded ALTEA-shield project discovered a dose equivalent rate reduction of 55 +/- 4% for a kevlar shield of 10 g/cm2. Polyethylene's performance was measured at 57 +/- 4%. The detector was set up in the Columbus module aboard the ISS and radiation data was recorded for the duration of experiement, recording the radiation levels during certain

times in the station's orbit. Due to the experiment occuring inside a module, radiation first interacted with the module hull before hitting the detector, changing the transport properties. The addition of Kevlar to spacecraft hulls can double as Micro-Meteroid Orbital Debris (MMOD) and radiation shielding (Narici, et al., 2017).

Another material (of sorts) which performs similar to polyethylene is the heat melt concept by Bahadori, Semones, Ewert, Broyan, & Walker, (2017), where space trash is melted, compacted into a brick-like shape and tested for it's radiation stopping power properties. Space trash is largely made out of plastics and this concept performed to 91 +/- 4.4% that of polyethylene against alpha particles with a kinetic energy of 207.8 MeV/n (Bahadori, Semones, Ewert, Broyan, & Walker, 2017). This illustrates the concept of utilizing onboard materials to construct a radiation sheild for the crew, which saves a tremendous amount of launch cost. Incorporating a similar design philosophy to include materials that serve a dual purpose will be beneficial to the spacecraft habitat design in this thesis.

A study optimizating material arrangement to affect radiation doseage was conducted by Sazali, Rashid, & Hamzah, (2018) and found little evidence to support this hypothesis. In fact, they went as far as to say that it was observed that there was no clear method on arranging the layers. Buildup factor was also found to be complicated in multilayer shields (Sazali, Rashid, & Hamzah, 2018). Furthermore, their review included shielding material combinations such as steel and polyethylene or polyethylene and lead. These shielding combinations would use thin layers of each material and sandwich them together, the result is a shield that is lighter in weight but performs as good or better at neutron slowdown than using strictly thick lead or steel walls. This review introduces flexible options for material placement around a spacecraft habitat, while still contributing equal effectiveness to radiation shielding.

Barthel & Sarigul-Klijn, (2017) provided an optimized solution for a radiation shielding architecture using polyethylene and varying the thickness of the radiation shield based on crew activities, for a 550 day Mars flyby mission. The optimization code allowed a mass decrease in the required shielding to decrease by 30% to achieve a dosage equivalent at the NASA permissible expoure limit (PEL) of 500 mSv/yr. The approach assumed the crew would spend cetain amounts of time in each compartment of the spacecraft habitat and adjusted the radiation sheilding based on these assumptions. The total mass of the radiation shielding was ~60 tons and the study validates the need to utilize more optimization techniques to provide the feasible approaches to the radiation protection challenge.

II.2 Systems Engineering Requirements

The spacecraft design requirements are informed by the literature review to drive the design to a feasible design concept. The spacecraft habitat design requirements are intended to provide guidance on baselined required solutions for the functions the spacecraft must provide. The first requirement communicates the spacecraft shall generate artificial gravity for crew usage. The spacecraft shall not exceed a maximum rotation rate of 6 RPM. The spacecraft habitat design shall not fall below the minimum tangential velocity requirement of 6 m/s. These constraints ensure the crew can successfully adjust to the rotational motion of the spacecraft while providing adequate outward force for the crew to stand on the floor.

The second requirement communicates the spacecraft habitat it shall set the maximum radiation exposure rate to 500 mSv/yr. This exposure limit is inclusive of the GCR dosage and any unexpected SPE dosages that could occur during the year. Furthermore, the spacecraft habitat shall only utilize passive radiation protection methods. Passive methods require no power source and ensure effective protection regardless of power issues that may occur during missions.

The third requirement communicates the spacecraft shall provide enough stowage to support a crew compliment for a maximum mission duration of three years. The three-year mission duration is an arbitrary duration that is used to give a constraint to the requirement. A three-year mission has the applicability to sending humans to the Moon, Mars and Venus.

The fourth requirement communicates the spacecraft shall incorporate technologies that have achieved a minimum TRL 6: system/subsystem model or prototype demonstration in a relevant environment (ground or space) (National Aeronautics and Space Administration (NASA), 2017) rating. This requirement ensures the technologies incorporated into the design assist to provide a feasible design solution.

Finally, the fifth requirement communicates spacecraft modules shall be built to the maximum dimensions of the current industry heavy lift launch vehicles and/or commercial cargo visiting vehicles to the ISS. If a situation arises where this is not achievable given the other requirements and constraints, then heavy lift launch vehicles that are currently in active development can also be considered. This ensures that the majority of modules are built to industry launch vehicle specifications, which offers flexible options for launching each module or part into orbit.

III REQUIREMENTS ANALYSIS

The research and requirements were analyzed to define a spacecraft habitat design. First, the spacecraft concept of operations are outlined to provide the scope of the spacecraft operations. Then artificial gravity actuation methods were analyzed to determine which is most suitable for this type of system. Finally, the space radiation countermeasures were developed utilizing simulations to define a minimum spacecraft habitat hull profile.

III.1 Spacecraft Concept of Operations

To understand the use for a reusable deep-space spacecraft, a concept of operations analysis is required. The focus is on the timing of visiting multiple celestial bodies for a human crew and what requirements need to be met in order to achieve this level of reusability and functionality. Trajectories for two missions, the first to Venus and the second to Mars are shown in Figure 9 below. The concept of operations in this example describes the spacecraft performing a mission to Venus (points 1-4) with a 30-day stay in the Venusian orbit, before arriving back to Low Earth Orbit (LEO). What follows is a period where the spacecraft undergoes cleaning, supply restocking and maintenance. The crew for the next mission, the Mars mission, also prepare for their mission during this time. The Mars mission is performed (points 5-8) for another 30-day stay in Martian orbit and the process can be repeated.

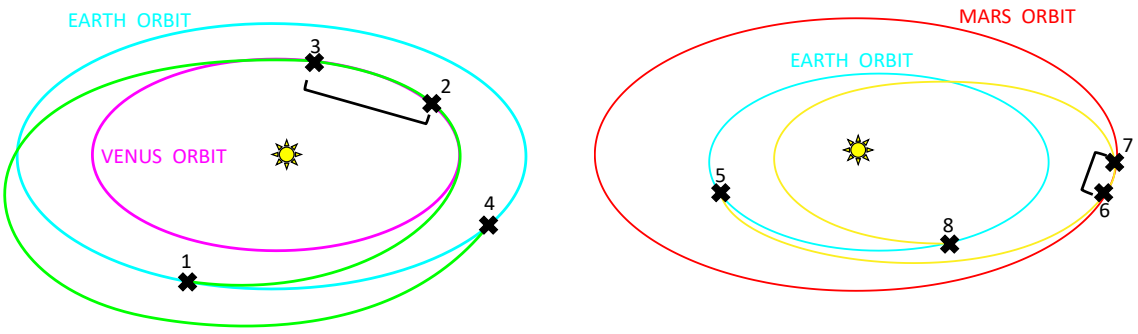

Figure 9: Multiple Mission Concept of Operations

Assumptions are made for mission duration and length, to ensure the human crew are exposed to the space environment for the least amount of time. Emphasis is therefore placed on shorter mission durations rather than longer ones. Based on shorter mission durations, it is also assumed a highly-sophisticated propulsion system capable of delivering up to 10 km/s of total delta-v (ΔV) for each mission. Finally, it is assumed that the spacecraft will spend approximately one year in a 200 km circular Earth orbit to prepare for the next mission. NASA's trajectory browser was utilized to understand the duration and ΔV characteristics of these types of concept of operations (NASA, 2016). Table 1 displays the mission dates for a human crew visiting two celestial bodies with mission lengths and estimated required ΔV:

Table 1: Departure/Arrival Dates for various celestial body missions

Destination	Earth Departure	Destination Arrival	Destination Departure	Earth Return	Stay time (days)	Duration (years)	Total ΔV (km/s)
Venus	Jun-02-2031	Sep-25-2031	Oct-25-2031	Aug-20-2032	30	1.22	5.61
Mars	Apr-12-2033	Oct-09-2033	Nov-08-2033	Jul-16-2034	30	1.26	8.3

The types of missions the spacecraft could perform for short stay times are payload delivery missions, exploration missions, passenger delivery missions or recovery missions. Payload delivery missions deliver payloads to planets where humans are planning on establishing outposts. The spacecraft could act as the transportation delivery system and provide a reliable means to efficiently deliver continuous payloads to a delivery site, with the intention of building up an outpost infrastructure.

Exploration missions are exactly as the name implies and a human crew could use the time to gather data on particular characteristics of the celestial body under investigation. Since a human crew would be directly at the observation site, quick decisions could result in more scientific discoveries and fast data processing. The potential for humans to perform directly in science missions while en route to and from a celestial is also invaluable, with the time having the potential to be utilized for deep space stellar observation, zero-gravity research, etc.

Passenger delivery missions could deliver humans to a new settlement outpost or include tourists on the journey, as part of an initiative to include more of the general public in space travel. These types of missions might be the most beneficial visiting the moon on a week or two week long journey as tourists get to experience space travel only previously experienced by a handful of humans. Recovery missions could also collect humans ready to travel back to Earth or aid in the recovery of damaged equipment vital to supporting and maintaining future outpost infrastructure. The importance of versatility and flexibility must remain in the design if a spacecraft if it is to performs complex operations such as the ones described here.

The high-level functions of the spacecraft were decomposed to analyze what functions are required for a multi-mission spacecraft. Although the spacecraft must be capable of performing a variety of functions based on the mission, the functional decomposition focuses on the high-level common functions performed, regardless of the mission the spacecraft embarks on. Upon performing this analysis, it is apparent that the spacecraft functions that share commonality within each mission is to perform orbit transfer (injection and escape) maneuvers as well as many system monitoring functions simultaneously. The spacecraft must also be prepared to engage in emergency procedures during a SPE and also perform trajectory course correction if the artificial gravity rotation misaligns the pointing vector. Figure 10 details the high-level spacecraft functional flow block diagram for a mission:

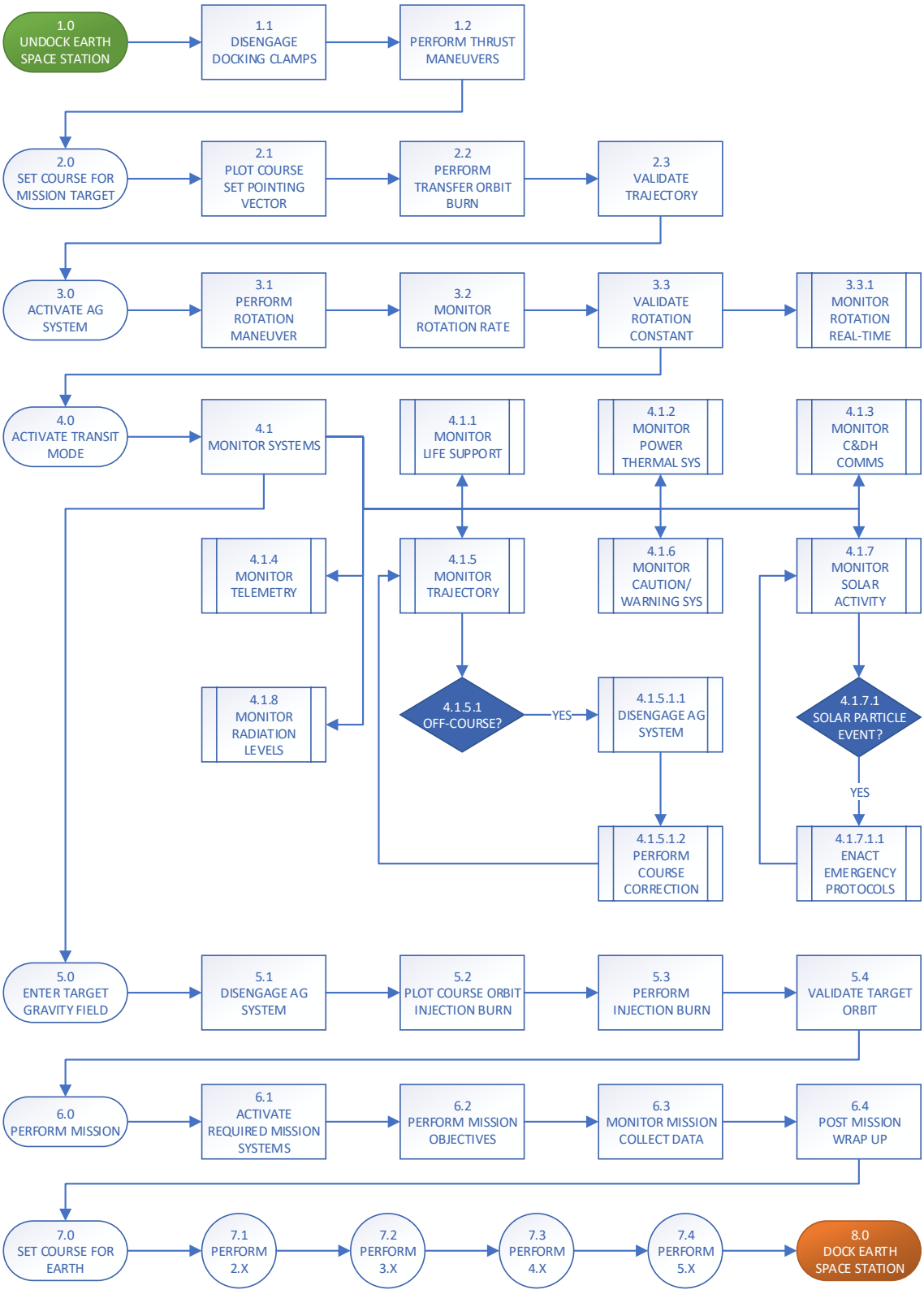

Figure 10: Spacecraft Functional Flow Block Diagram

An analysis of the capabilities of current and near-term launch vehicles was conducted to ensure the compatibility of the spacecraft habitat design would fit into most payload fairings. Table 2 below identifies the internal dimensions of six payload fairings and their maximum launch mass to LEO.

Table 2: Internal dimensions and launch mass capacity of launch vehicles
(Arianespace, 2016) (United Launch Alliance, 2010) (United Launch Alliance, 2013) (SpaceX, 2019) (Blue Origin, 2018) (NASA, 2018)

Vehicle	Internal Diameter (mm)	Cylindrical Height (mm)	Max Height (mm)	Mass to LEO (kg)
Ariane 5	4,570	10,039	15,589	7,000
Falcon 9	4,600	6,700	11,000	10,886
Delta IV	4,572	11,034	15,761	28,790
Atlas V	4,572	12,192	16,484	29,400
New Glenn	6,228	10,520	17,632	45,000
SLS Block 1B	7,500	9,860	16,510	95,000

For full compatibility with all these launch vehicles, the majority of spacecraft components will be required to fit inside these payload fairings. This is a constraint applied to the external diameter of the spacecraft habitat components. The cylindrical height is defined as the height of the payload fairing before the fairing begins to taper into a curved shape. From the table, the maximum diameter is 4,572 mm with a height of 6,700 mm. Not all components will meet these dimension requirements, but designing to these specifications will ensure the optimal compatibility for components. This also ensures that there is no single fault tolerance for launch vehicles, as not all launch vehicles have had 100% success rates. Designing to account for many options ensures the greatest chances of success for construction.

III.2 Artificial Gravity Research

III.2.1 Analysis

To define functional volumes from an artificial gravity perspective, considerations must be made for which topology to select as the baseline configuration. Given the radii required to establish an artificial gravity system for humans is at least one order of magnitude

larger than the humans that will be occupying it, an examination into the current space habitats is necessary to establish a baseline design. The ISS modules have an internal diameter of approximately 4 m, which also include volume allocation for utilities and equipment racks. Crew are able to maneuver through the modules without impedance and the internal volume is not too large that crew members find the space unusable. Due to the microgravity environment, traversing through a space with excessive volume would not trouble the crew. In an artificial gravity environment, the plane of motion becomes constrained and excessive volume is something to consider and ensure there is not too much of it in the design.

Functional volume can be defined as the volume in which a human crew member has good accessibility to all the internal systems that surround them, with little effort to reach those hard to reach areas. Although this is highly qualitative, we can more clearly define a quantitative functional volume by using a cross section analog of the ISS internal module volume, defined by Figure 11 below:

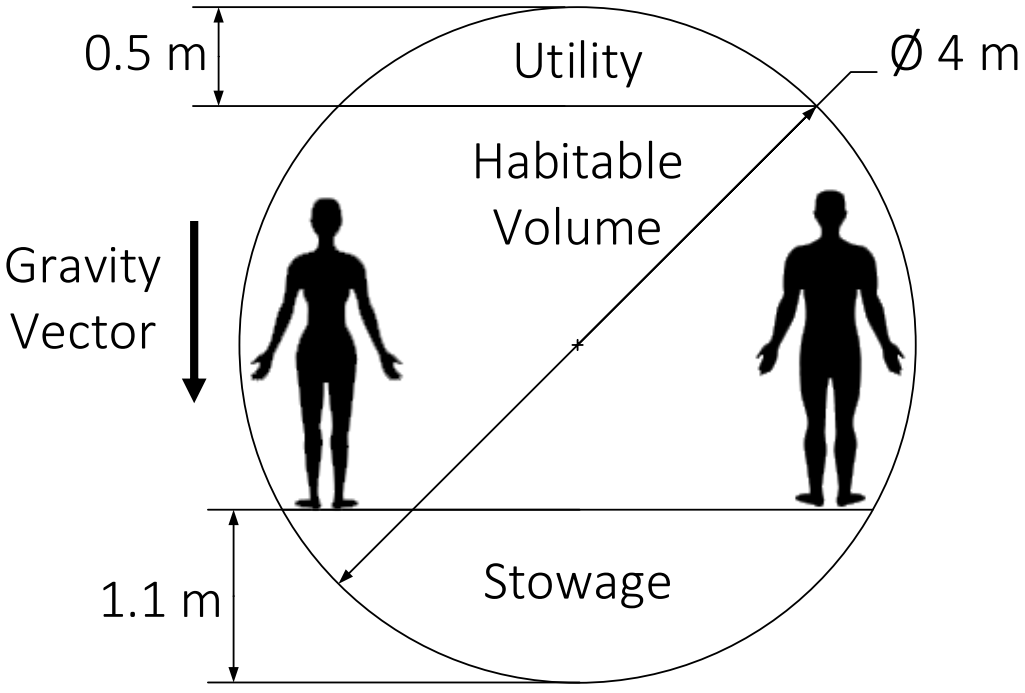

Figure 11: Baseline Habitat Functional Volume Cross-Section

Assuming the crew wish to experience equal artificial gravity levels for the duration of their mission, the floor must exhibit isotropic properties relative to the center of rotation. Therefore, the volume is constrained by the circular module and further constrained by roof and floor structures, which help the crew to work within an artificial gravity environment.

The torus shape is able to confine the useable volume to a specific radius, it is quite a large and unwieldy shape and in its current state it is not able to be launched by conventional methods. For this reason, if a torus shape is to be utilized, then it must made from a flexible material and split into sections to meet the launch vehicle payload fairing requirements. The use of wound inflatables is a feasible solution, as there is research to suggest this technology is possible (Harris & Kennedy, 2000). When considering which to use, an analysis between the useable volume and radius was conducted.

Based on the SpinCalc calculator, the angular velocity, tangential velocity and centripetal acceleration (Hall, SpinCalc, 2018). Table 3 identifies the three cases evaluated, at 10 m, 15 m, and 20 m. The red values indicate values that are considered outside of the bounds established by the literature.

Table 3: Rotational kinematics for potential artificial gravity radius candidates

Radius (m)	Ang Vel (rpm)	Ang Vel (deg/s)	Tan Vel (m/s)	Tan Vel (km/hr.)	Centripetal Acc (g)	Centripetal Acc (m/s^2)
10	6	36	6.28	22.62	0.4	3.95
	5.73	34.38	6	21.6	0.37	3.6
	5.12	31.08	5.42	19.53	0.3	2.94
15	6	36	9.42	33.93	0.6	5.91
	5	30	7.85	28.27	0.42	4.11
	4.23	25.37	6.64	23.91	0.3	2.94
	4	24	6.28	22.62	0.27	2.63
20	6	36	12.57	45.24	0.81	7.9
	5	30	10.47	37.7	0.56	5.48
	4	24	8.38	30.16	0.36	3.51
	3.66	21.97	7.67	27.61	0.3	2.94
	3	18	6.28	22.62	0.2	1.97

Table 4 shows a volumetric analysis conducted at the three radii cases to determine the volume and surface area afforded by the topology, with an integrated floor and roof.

Table 4: Functional Toroidal Volume and Area analysis

Radius (m)	Volume (m^3)	Surface Area (m^2)	Surface Area (ft^2)
10	718	224	2,411
15	1,113	337	3,627
20	1,508	449	4,833

A study into the minimum net habitable volume was conducted for a return mission to mars by a Johnson Space Center (JSC) NASA team. The assumption was based on the crew operating in zero-gravity for the mission duration. Also, in the discussion noted the longer the mission, the more volume the crew is likely to require for psychological reasons (Whitmire, et al., 2015). Table 5 provides an estimate for how much volume each crew member required, based on this research. Table 6 calculates the maximum crew size and the volumes associated, based on the aforementioned net habitable volume study and applying assumptions made to the torus geometry:

Table 5: Assumptions for Habitat Volume Sections

Crew Quarters (m^3)	Workspace (m^3)	Exercise (m^3)	Dining (m^3)	Recreation (m^3)	Hygiene (m^3)
9	4	3	50 (2 Modules)	4	50 (2 Modules)

Table 6: Volume analysis of habitat spaces

Radius (m)	Max Crew Size	Crew Quarters (m^3)	Workspace (m^3)	Exercise (m^3)	Dining (m^3)	Recreation (m^3)	Hygiene (m^3)
10	13	117	52	39	50	52	50
15	23	207	92	69	50	92	50
20	34	306	136	102	50	136	50

There are many methods to feasibly generate artificial gravity conditions through rotational motion. The literature has shown the use of propulsive means through chemical or electric thrusters as well as the use of motors to rotate surfaces. Since propulsive methods have been thoroughly explored, this analysis provides an analysis on an alternative method of

generating an artificial gravity environment. This is through the integration of a linear induction motor internal to the habitat. This analysis was performed to determine how feasible this system is, based on the preliminary work by Zipay, (2019). Figure 12 identifies the trade space for generating the centripetal forces inherent to producing the artificial gravity conditions aboard a spacecraft.

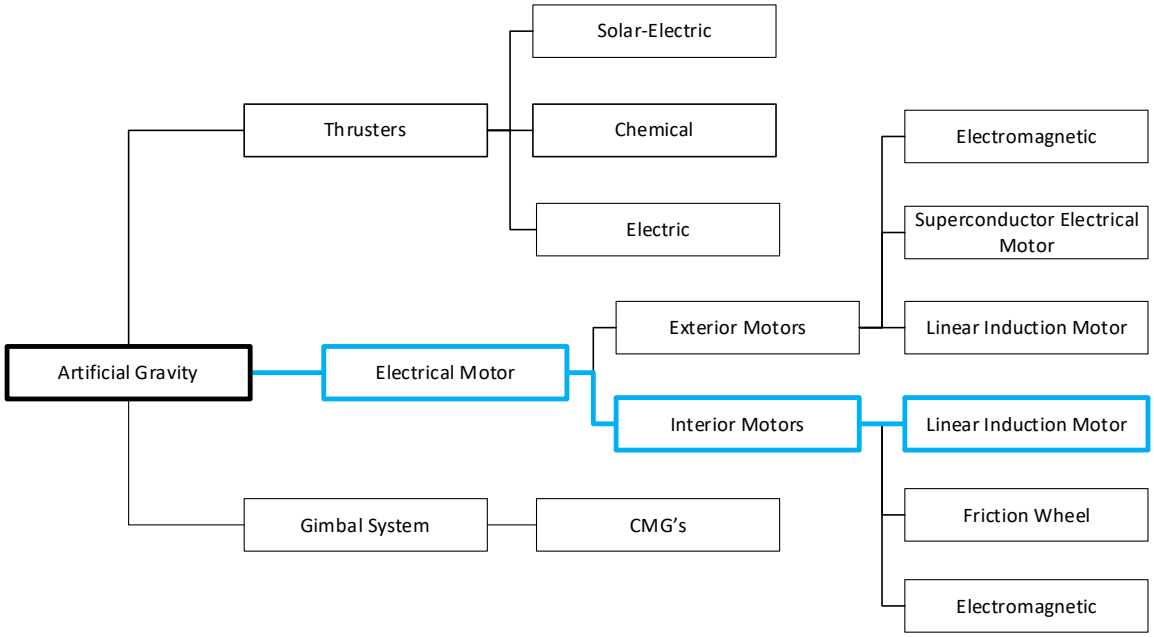

Figure 12: Artificial Gravity Actuation Trade Tree

An internal induction motor system is appealing for this type of spacecraft as it provides artificial gravity to the crew without propellant and the supporting subsystems associated with thruster systems. To fully analyze if this concept is feasible for the spacecraft design, an analysis of the physics involved as well as what systems are required to support the internal induction motor system is required. An examination of the mechanical forces that act on the rotating platform during rotation was performed. Since the design of the platform is analogous to a ball bearing, two forces were identified: radial forces and thrust forces. Radial forces are forces identified to be primarily created by the crew through motion, whereas the thrust forces will be created most likely from external sources such as spacecraft movements.

Figure 13 demonstrates the effect on the center of rotation radial and thrust forces have on the rotating platform. If the platform is not aligned or secured to the inner hull then undesirable motions of the platform will occur. Misalignments such as this pose potential hazards for crew in the form of disorientation and motion sickness as well as mechanical damage to the surrounding hardware. Platform misalignments due to uneven forces during rotation are also shown in Figure 14. Radial forces (shown in red and orange) could cause the platform to wobble during rotation. Prolonged unresolved wobbling leads to resonant motions which can cause the entire structure to move in unsought vectors. Resonant motions have observed on the ISS during astronaut exercise periods. A force absorption mechanism and platform alignment system are required to keep the platform steady during rotation and to absorb radial forces generated by the crew during operation.

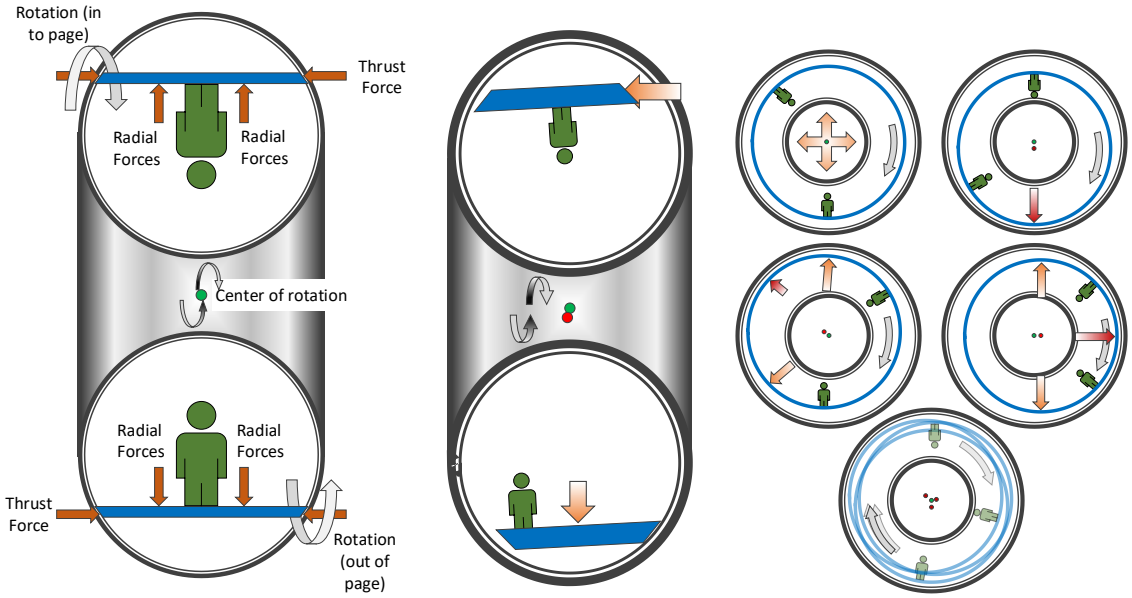

Figure 13: Forces Acting on Rotating Platform (left), Uneven Forces Acting on Platform (middle), Precession Effects (right)

A shock and vibration assembly must absorb the forces generated by the occupants whenever they are exercising or moving large objects. During running, the average human can generate up to 4,700 newtons of force (Birnbaum, 1999), or approximately 470 kgs, per foot

strike. Mechanisms are required to absorb at least this amount of force while the crew perform running or cardio activities. Suspension systems as seen on cars are a likely candidate solution for a force absorption mechanism. Also, vibration isolation hardware is also examined due to the high number of applications in a wide spread of industries, from defense to aviation to sensitive scientific experiments.

The steel cable vibration isolation hardware was by far the most compelling in terms of simplicity and ability to absorb forces. Depending on the design of the hardware, the devices can handle up to 50,000 newtons of force (Vibro/Dynamics LLC, 2018) and be able to handle loads from different directions. Standard car shock absorbers are excellent for handling shock in one direction but are not suited for omni-directional forces. Based on Figure 14, a shock absorption mechanism must be capable of absorbing forces from multiple force vectors.

Materials research was conducted to determine the composition of the platform component in order to ascertain the mass properties. The platform has two major requirements: maximize mass reduction and to provide adequate support to the crew and equipment during artificial gravity operations. Lightweight materials with high tensile and shear stress values fulfill these requirements.

The investigation explored deployable platform concepts used in concert staging and various types of wood/metal configurations for outdoor applications. The decks of airplanes were also investigated leading to carbon fiber composites research. These composites are utilized both the aerospace and space industries and are comprised of an aluminum honeycomb sandwiched between two sheets of carbon fiber. The manufacturing processes are standardized and the application of these materials are well understood. More importantly carbon fiber composites have some of the lowest mass to volume ratio's, while still providing incredible amounts of tensile strength.

Analysis of Coriolis forces is important to understand how the artificial gravity environment will impact the crew, as well as what activities the crew must be prepared to compensate for as the effects occurs during periods of rotation. The governing equation for describing the forces acting on a body in a rotating reference frame is

$$F' - m\frac{d\Omega}{dt} \times r' - 2m\Omega \times v' - m\Omega \times (\Omega \times r') = ma', \quad (1)$$

where F' is the sum of all the physical forces acting on the body relative to the rotating reference frame, m is the body mass, a' is the body acceleration in the rotating reference frame, Ω is the rotation vector, t is time in seconds, v' is the body velocity in the rotating reference frame and r' is the body position vector in the rotating reference frame.

The Coriolis force is described as

$$2m\Omega \times v', \quad (2)$$

which indicates that the Coriolis force is dependent on the body's velocity vector relative to the rotation vector.

Crew members walking along the longitudinal axis of the habitat, which is along the length of the rotation axis experience no Coriolis forces since the change in velocity with respect to the rotating reference frame is zero. Interestingly, a crew member walking along the transverse axis, which is walking around the curved surface experiences a Coriolis force orthogonal to the rotation axis. This gives the crew member an "additional force" to contend with when traversing across the surface. If the crew member walks with the direction of rotation, they experience the summation of the Coriolis force and centripetal force, experiencing a gain in perceived weight. However, if the crew member walks against the direction of rotation, they will experience the subtraction of the Coriolis and centripetal forces, making them feel "lighter". This is due to the crew member increasing or decreasing their tangential velocity as they walk across the surface.

Increasing the tangential velocity increases the crew member's rotation rate with respect to their coordinate frame and the opposite effect occurs when decreasing the tangential velocity. It is unclear based on the current understanding of the literature if the comfort levels would be affected by crew members walking around. Crew members that are in a 6 RPM rotating habitat are already at the maximum RPM as indicated by the literature (Hall, Artificial Gravity in Theory and Practice, 2016), to have this increase further due to a crew member walking about the habitat could cause unforeseen discomfort. A remedy for such a situation is to increase the radius of the habitat while decreasing the total RPM to account for crew movement when walking in the direction of the rotation. Another remedy is to restrict crew movement to only walking in the opposite direction of rotation, however this presents its own challenges as crew members will experience less "force" to keep in contact with the surface and thus negate the perceived centripetal forces altogether, almost undoing the premise of a rotating structure to produce artificial gravity. Table 7 shows the Coriolis forces for walking and jogging movements at 1.5 m/s and 2.5 m/s respectively. These numbers are for the magnitude only, however if a crew member is walking with the rotation the number is positive, if they walk against the rotation the number is negative.

Table 7: Coriolis force magnitudes (newtons) of crew traversing rotating surface

	6 RPM	**4 RPM**	**2 RPM**
Walk 1.5 m/s	132.2	88.2	44.1
Jog 2.5 m/s	220.5	147	73.5

Figure 16 describes a use case scenario where a crew member with a mass of 70 kg performs walking movement at 1.5 m/s and jogging at 2.5 m/s. The net force is the summation of the Coriolis and centripetal forces acting on a moving crew member in the rotating reference frame. Since the centripetal force increases with increased radius and ensuring walking and jogging velocities are constant, the crew member can expect to see an

increase in net force acting on them while walking/jogging in the direction of rotation, and a decrease in net force when moving against the direction of rotation.

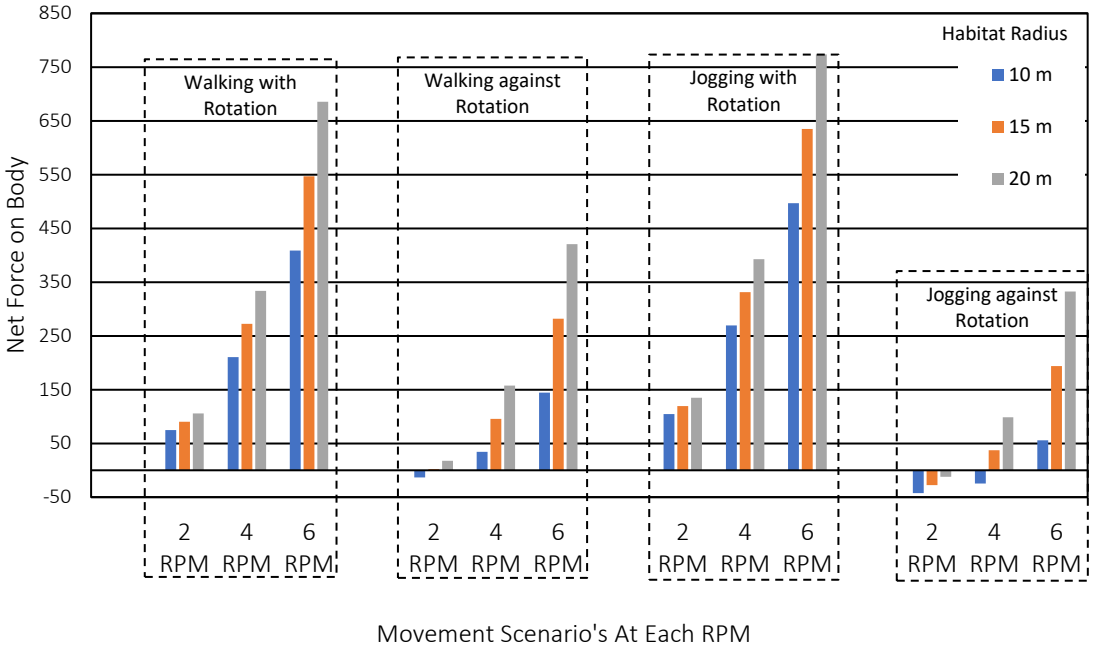

Figure 14: Net force acting on body at varying movement velocities and RPM's

The same is true for crew members moving toward the rotation axis, as they will experience a Coriolis force pushing them to the left of right, depending on their own coordinate frame. The magnitude is less than that of a crew member walking on the rotating surface as traversing in the crew member's perceived "up" direction will require equipment such as a ladder to do so. Since traversing a ladder is assumed to be about 0.5 m/s, this is one third that of the walking speed, so the magnitude of the Coriolis force acting on the crew member climbing a ladder will be also one third. The direction of the Coriolis force changes though, with respect to the crew members reference frame the direction will be perceived to be pushing them to the left of right.

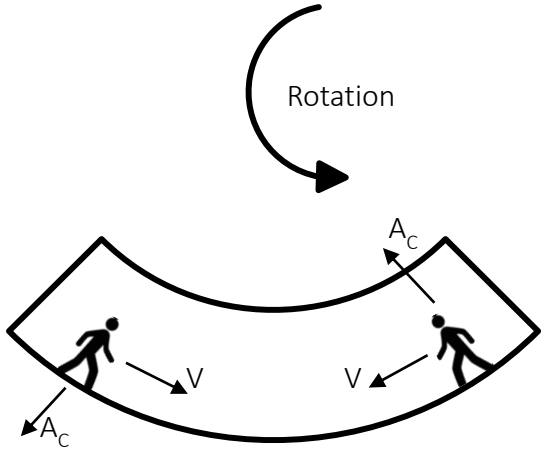

Figure 15: Forces acting on walking crew members

Coriolis forces might be a disruption to the crew until they become acclimated to the environment. The assessment of Coriolis forces can inform future design solutions for rotating habitats. The magnitude of the Coriolis force increases and decreases depending on the velocity vector of the crew member and its direction is dependent on the velocity vector's direction with respect to the primary rotation axis. Figure 18 describes the motions the crew experiences during climbing a ladder towards or away from the center of rotation.

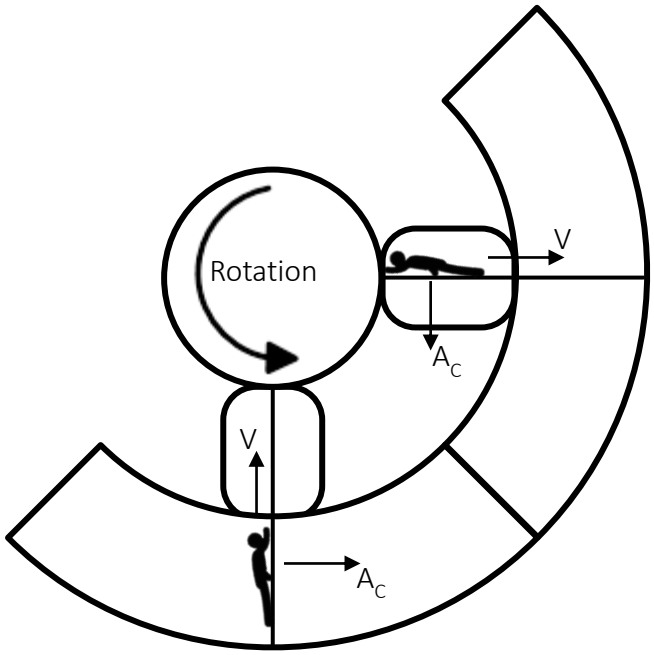

Figure 16: Forces acting on ladder climbing crew members

III.2.2 Design Results

The module follows a similar design configuration and material composition to the modules that currently comprise of the ISS, with the outer diameter measuring 4.57 m with an inner diameter of 4.2 m, and a length of 4.0 m. The module will have both ends open with an inflatable interface seal on one side and a permanently mounted inflatable on the other side. The top of the module accommodates a passive Common Berthing Mechanism (CBM) connecting to other modules. The configuration utilizes four of these modules, each accompanied with an inflatable section that spans for one quarter of the entire circumference of torus. The end of the module that interfaces with the inflatable requires a specifically shaped and hardened interface to handle the compression loads that are exerted by a marman clamp, which is designed to create the atmospheric seal. The module interior includes all the mounting hardware preinstalled for the platform alignment bearings and a linear induction motor (LIM) locomotive system. The alignment bearings sit on L-brackets that are be connected to the interior hull. Figure 18 visualizes the module design for integrating a LIM.

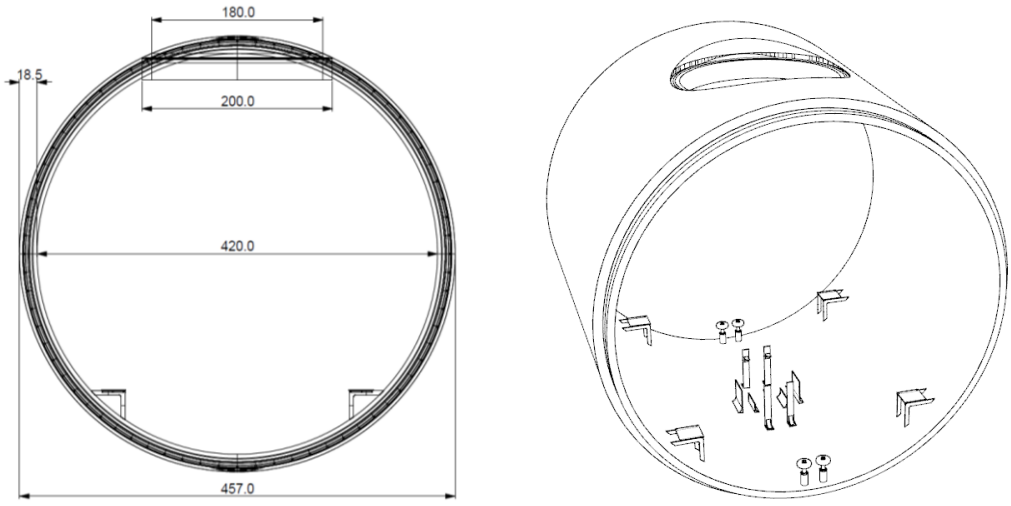

Figure 17: Module dimensions (left). Module with hardware mounts installed (right).

The alignment bearing assembly serves three purposes: ensure correct platform alignment during rotation; absorb the instantaneous forces generated by the crew during

rotation; isolate the platform vibrations from the rest of the spacecraft. The assembly consists of a large ball bearing similar to element roller bearings used in many applications from skateboard wheels to car bearings. These bearings are able to handle both radial and thrust forces and be lightly greased to lower the friction coefficient. The ball bearing will sit inside a socket enclosure to prevent the bearing from popping out of the assembly. The lower half of the assembly will house the vibration isolation hardware in the form of steel cables. The circular design of the cables provides omni-directional force vibration and absorption. A configuration such as this can handle forces up to 50,000 newtons (Vibro/Dynamics LLC, 2018). Four bearing assemblies are installed per module and could potentially absorb up to 200,000 newtons of force, equivalent to 40 crew members running simultaneously.

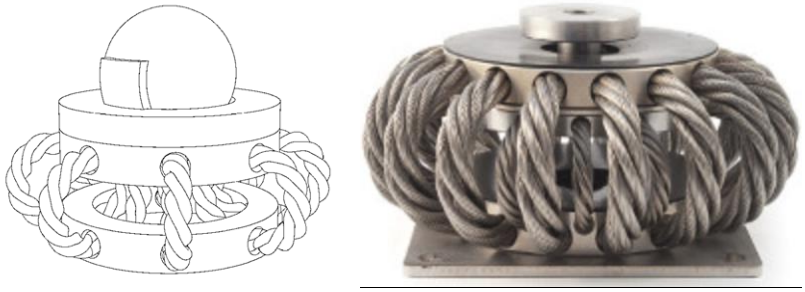

Figure 18: Model of shock absorption assembly (left). Anti-vibration/shock mount (right) (Vibrostop, 2018).

The platform design is curved to maintain the crews position with the rotational axis. The platform is comprised of two sheets of carbon fiber at 3 mm thick, with the aluminum honeycomb sandwiched between them. The bottom sheet has two grooves that will run along the alignment bearing assembly. The sides of the platform are made of aluminum beams and allow adjacent platforms to connect to each other using standard nuts and bolts. The threads will utilize helicoils in order to prevent thread stripping. Curved triangular aluminum beams will run perpendicular to the aforementioned aluminum side beams for a little added structural

support and provide an interface to adhere the carbon fiber sheets to. Additional mounting holes will run along the sides of the platform to mount the walls to the platform.

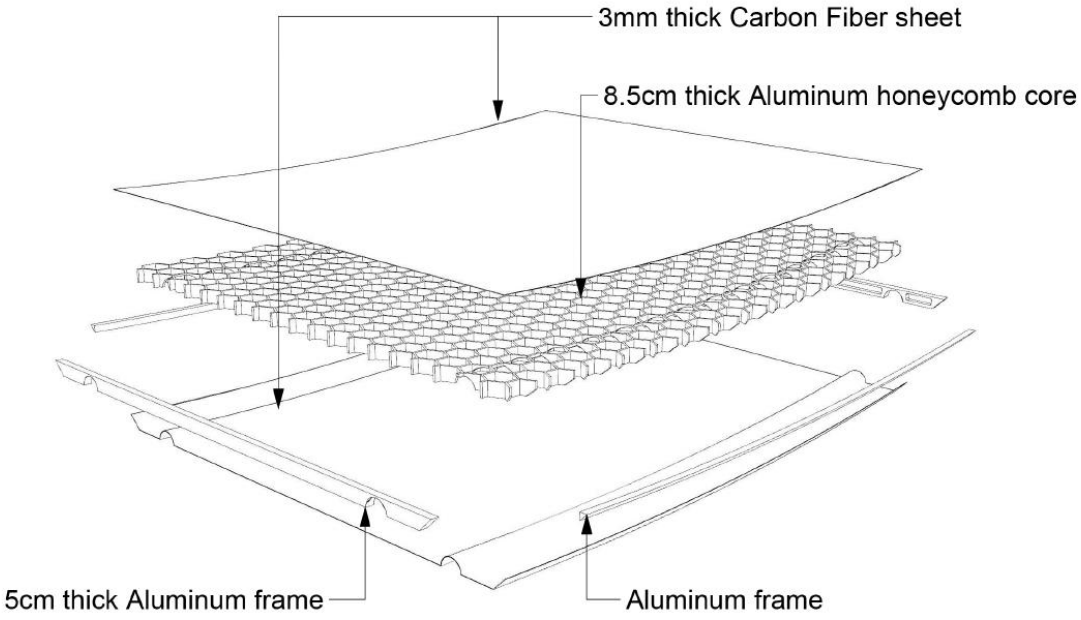

Figure 19: Platform Components.

The locomotion assembly consists of the LIM and the brake system. The LIM is comprised of copper coils that generate the required magnetic fields. The brake system is comprised of two solenoids with armatures that hold the braking pads. Retention springs keep the discs engaged when no power is applied. In order for the brakes to disengage, enough power must be applied for the solenoid to overcome the spring tension from the retention springs. This ensures that during a power failure the brakes are automatically be applied through passive mechanical methods, improving reliability and reducing maintenance.

The rotor for the LIM is constructed of solid aluminum, which is non-metallic and is a proven material for LIM rotors (Dodson, 2013). The holes in the rotor are to reduce the rotor mass and due to the rotation speed; the LIM will not need to interact with every part of the rotor. This design is subject to change if and when a more rigorous study is required for

the design and manufacturing of the rotor. At the bottom of the rotor is the rotor contact for the braking system, which will be made from a carbon fiber composite material. Near the ends of the module are guide wheels that help to maintain the orientation of the rotor and platform if any forces try to misalign the entire structure.

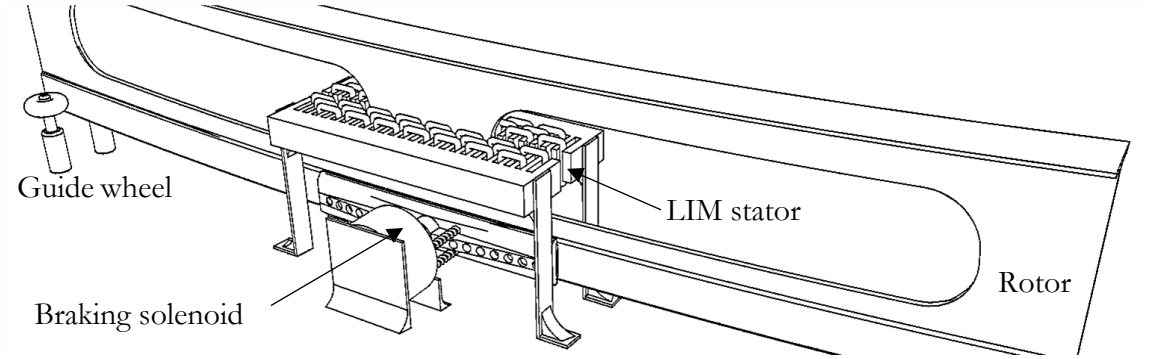

Figure 20: Linear Induction Motor System

Figure 18 shows the relationship between the mass of the platform assembly and the time taken to achieve 6 RPM for a 24.8 m radius assembly. Calculations were made for cases from 40 tons to 100 tons, it is worth noting power generation below 10 kW is achieved at ~ 900 seconds (15 minutes) for the 40-ton case and ~ 2200 seconds (37 minutes) for the 100-ton case. Although the mass of the platform increases, even very large masses are still able to able to achieve 6 RPM with conservative power, given enough time. Each module is assigned a LIM assembly, decreasing the power per motor by a factor of four. It is worth noting electric trains have masses on the order of hundreds of tons and are able to be operating entirely utilizing a system similar to this, therefore the feasibility of such a system is sound.

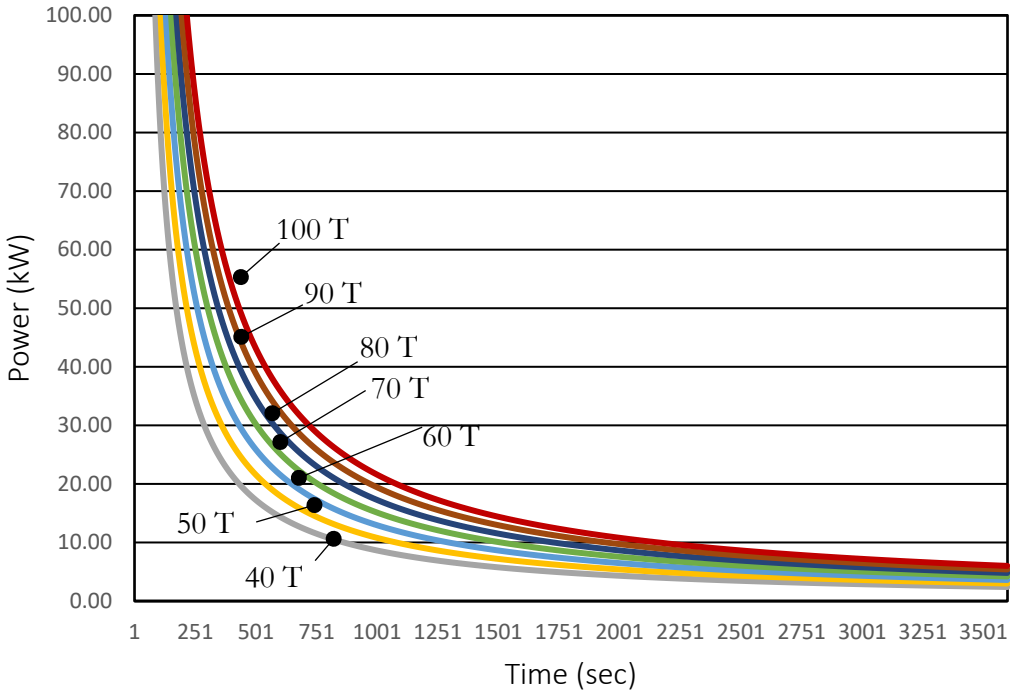

Figure 21: Power required per unit time to reach 6 RPM for 24.8 m radius

III.2.3 Discussion

The concept of an internal rotating assembly is a departure from the majority of articles this author was able to find. The assembly allows the spacecraft to actuate a rotating platform that can be controlled electronically, eliminating the need for fuels and the supporting propulsion sub-systems. Furthermore, the assembly is contained internally and allows the crew to start and stop the platform as required to access other parts of the spacecraft.

The purpose to investigate this concept was to determine if it would prove useful in further conceptual designs, as the literature is devoid of such internal rotating platform designs. However, it is a complex system and safety issues related to rapid decompression do not have straight forward solutions with this design. The application of the internal rotating platform in a mobile multi-mission spacecraft doesn't present itself as the most feasible

solution due to these complexities. However, the platform design itself can be incorporated into a static assembly with a spacecraft habitat rotating utilizing external propulsive forces.

III.3 Space Radiation Research

Humans currently living and working in space are exposed to high levels of space radiation due to hostile space environment and inadequate radiation protection. There exists a need for habitat design solutions that quantitatively provide enough radiation protection to prevent long term radiation illnesses. This section intends to provide a practical design solution incorporating As Low as Reasonably Achievable (ALARA) principles that integrate adequate radiation protection into a spacecraft hull assembly to provide sufficient protection from space radiation to the crew. The evaluation scope is the predominate layers that compose a spacecraft hull, both for hard-shell modules and soft-shell (inflatable) modules; it does not account for structural items such as standoffs nor low density materials or extremely thin materials utilized.

The NASA Human Research Program (HRP) identifies radiation as a primary hazard for human spaceflight, while also acknowledging deep space journeys/habitation require mitigating approaches to ensure the long term health of space-faring crew's (National Aeronautics and Space Administration (NASA), 2019). Furthermore, radiation shielding solutions must stay within a 95% allowed risk limit for Permissible Exposure Limits (PEL's); current estimates show females and males of 35 years of age to be exposed for 154 and 216 days respectively outside of low-earth orbit (National Aeronautics and Space Administration (NASA), 2019). Material research is required to reduce the effective dosage to humans in deep space. Shielding physics and dosimetry is one of the mitigation strategies for radiation protection and the development of the High Charge and Energy Transport (HZETRN) code is a step towards that. On-Line Tool for the Assessment of Radiation in Space (OLTARIS) is a web-based integrated toolset utilizing HZETRN transport codes and this tool allows the

quick evaluation of spacecraft structures (Singleterry, et al., 2010). Using the NASA PEL of 500 mSv/yr. and OLTARIS evaluation tool, it is possible to develop and evaluation possible spacecraft hull configurations that meet the requirements for providing adequate radiation protection for long term deep space manned missions.

III.3.1 Methods

A holistic approach was performed to inform of potential spacecraft hull designs that met the requirements: reduce the annual exposure dosage to below 500 mSv and provide a hull design that is light enough be to launched with current launch vehicle capabilities. To begin, research was conducted to determine an approximate model of spacecraft hull configurations for both hard- and soft-shell configurations. Micro-Meteoroid and Orbital Debris (MMOD) configurations which aided in the retrieval of the material utilized but also their thicknesses were retrieved from NASA technical reports server (Christiansen & Lear, 2012). Furthermore, Transhab radiation protection laboratory measurements were conducted to determine and characterize the MMOD capabilities and radiation countermeasures for the Transhab inflatable while in Low Earth Orbit (LEO). The work detailed the layers that built up the inflatable shell of Transhab (Badhwar, Huff, Wilkins, & Thibeault, 2001). Table 1 details the baseline hull configurations for the hard- and soft-shell modules to approximate for radiation simulation:

Table 8: Baseline Hard Shell and Inflatable Module Composition Assumptions

	Function	Material	Layer Thickness (mm)	# Layers	Total Thickness (mm)
Baseline Hard Shell Module [?]	MMOD Exterior Bumper	Aluminum	3	1	3
	Thermal Insulation	Mylar	0.127	20	2.5
	MMOD Intermediate Bumper	Nextel	1.4	6	8.4
	MMOD Intermediate Bumper	Kevlar	0.35	6	2.1
	MMOD Rear Wall / Pressure Vessel	Aluminum	5	1	5

Baseline Inflatable Module [?]	Exterior Thermal Insulation	Mylar	0.42	1	0.42
	MMOD - Intermediate Bumper	Nextel	1.12	12	13.44
	Restraint Layers	Kevlar	1.07	14	15
	Redundant Bladders	Armor Flex (LDPE)	0.3	11	3.35
	Inner Bladder	Nomex	3.175	1	3.175

Due to the large number of layers, the Transhab inflatable module composition was approximated by combining the layers and materials that were regularly repeated throughout the structure. Figure 1 shows the complex layer system the Transhab module is composed of. Materials that occurred a single time and were extremely thin (such as Beta Cloth, 0.2 mm thickness) (Finckenor & Dooling, 1999) were excluded due to the assumption they would have minimal impact on the radiation simulations. Also, materials that lacked substantial density such as the polyethylene foam layers with a total thickness of 406 mm but potential densities of 0.025 – 0.185 g/cm^3 (Biron, 2017) were also excluded as the one to two orders of magnitude density reduction is assumed to afford minimal contributions to the simulation results. Mylar is the primary material for MLI, so it was assumed to be the prime contributor to the radiation transport simulation results.

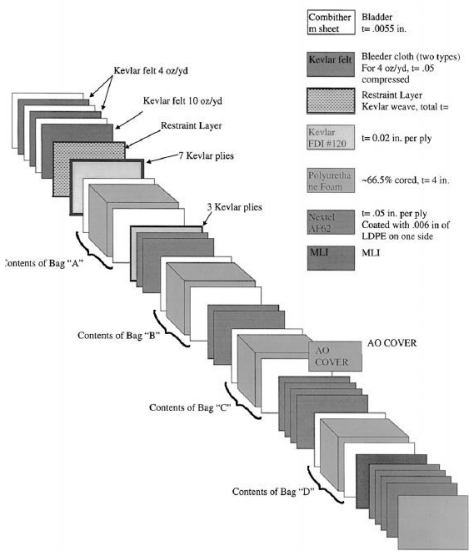

Figure 22: Layer Composition of the Transhab Module (Badhwar, Huff, Wilkins, & Thibeault, 2001)

The baseline hard- and soft-shell configurations were evaluated in OLTARIS to establish their performance within the simulation parameters. The simulations consisted of two tests, one GCR and one SPE. The GCR simulation ran the Badhwar-O'Neill 2014 model in free space at 1AU, setting the mission definition to the 2010 Solar Min since GCR is the strongest during minimum solar activity. The SPE simulation ran the historical SPE data of three SPE events that occurred during August – October 1989 in free space at 1AU. The objective is to assume a worst-case scenario for a spacecraft operating in deep space with not enough time to travel back to Earth for protection. If a similar future event occurs, it is likely the spacecraft and its crew would encounter this scenario and adequate SPE countermeasures are required to prevent the crew from the aforementioned side-effects from chronic SPE exposure.

All hull configurations were assumed to resemble a spherical geometry with the dosage calculated from the radiation fluences recorded at the center of sphere. This dose is applied to a tissue simulant which produces the dose equivalent data. The simulation results are focused on the worst-case dose equivalent (solid cancer) results. Table 2 shows the baseline results for GCR and SPE dosages using OLTARIS:

Table 9: Baseline Hard Shell and Inflatable Module OLTARIS Results

	GCR Dosage (mSv/yr.)	SPE Dosage (mSv/yr.)	Total Areal Density (g/cm^2)
Radiation Dosage No Shielding	810	853,600	N/A
Baseline Hard Shell Module	681	7,636	508
Baseline Inflatable Module	579	3,782	662

The baseline simulations provide a comparison between what is currently utilized in the space environment and the space radiation levels that must be protected against. The GCR dosage is 36.2% above the maximum allowable limit while the SPE is three orders of magnitude higher than the maximum allowable limit. Despite the extreme radiation levels

created by SPE's, the ability for the modules to reduce the dosage by two orders of magnitude gives us confidence that an achievable solution is possible.

Based on the baseline simulation results various configurations for both hard- and soft-shell modules were considered for the introduction of alternative materials for module construction. The general hull composition for both module types remained as too much deviation from the baseline could lead to unverifiable results. The performance for each was evaluated on their GCR and SPE dose equivalent results and through each configuration, slight iterations were made to either increase the primary radiation protection layer thickness or to increase the thicknesses of the surrounding structure.

Once suitable configurations were found, a design mockup of each hull configuration was modelled to examine the mass properties and determine feasibility for launch. Generalized hull dimensions were utilized, similar to current module configuration on the ISS.

III.3.2 Results

The proposed hard-shell module design incorporated carbon fiber composites into the structure, as well as increasing the number of layers of Kevlar. The decision to use carbon fiber composites over aluminum was based on prior research showing it outperforms aluminum for radiation protection while decreasing overall mass since carbon fibers density is 45.2% less dense than aluminum. Additional Kevlar layers increased the areal density from 30.2 to 121.0 g/cm^2 but does not increase the overall thickness of the spacecraft hull as the Kevlar is in a gap between the outer bumper and rear wall. This increase in Kevlar mass is offset by the decrease in pressure vessel mass due to the introduction of carbon fiber. The outer bumper remained aluminum as it was recommended by NASA to use a metal for this part (Christiansen & Lear, 2012).

The proposed soft-shell module design did not see any changes other than the addition of the radiation protective elements. Due to its recent emergence into the space industry, this technology is still under evaluation and testing. Both the hard- and soft-shell modules were evaluated with the addition of a polyethylene radiation protection layer of varying thicknesses from 50 to 400 mm. The highlighted rows in Table 3 indicate the changes for each module. Table 3 provides the composition of these layers evaluated in the simulations:

Table 10: Proposed Hard- and Soft-Shell Modules for Increased Radiation Protection

	Function	Material	Layer Thickness (mm)	# Layers	Total Thickness (mm)
Proposed Hard Shell Module	MMOD - Exterior Bumper	Aluminum	3	1	3
	MMOD - Intermediate Bumper	Nextel	1.4	6	8.4
	MMOD - Intermediate Bumper	Kevlar	0.35	24	8.4
	MMOD - Rear Wall	Carbon Fiber Composite	5	1	5
	Radiation Shield	Polyethylene	50-400	1	50-400
	Thermal Insulation	Mylar	0.127	20	2.5
	Pressure Vessel	Carbon Fiber Composite	3	1	3
Proposed Inflatable Module	Exterior Thermal Insulation	Mylar	0.42	1	0.42
	MMOD - Intermediate Bumper	Nextel	1.12	12	13.44
	Radiation Shield	Polyethylene	50-400	1	50-400
	Restraint Layer	Kevlar	1.07	14	15
	Redundant Bladders	ArmorFlex (LDPE)	0.3	11	3.35
	Inner Bladder	Nomex	3.175	1	3.175

The GCR dosage for the proposed modules is shown in Figure 1, and the SPE dosage for the proposed modules are shown in Figure 2. Polyethylene as a standalone material was evaluated alongside the proposed hard- and soft-shell modules for comparison purposes. The figures red line indicates the 500 mSv/yr. PEL while the black boxes surrounding specific data points indicate the radiation shield thickness of 100 – 200 mm for GCR and 350 – 400 mm for SPE.

These thicknesses provide adequate radiation protection while allowing for a feasible launch mass. Due to GCR's persistent nature, protection from this type of radiation takes precedence. Therefore, since the data indicates that 100 mm of radiation protection reduces the whole-body tissue dosage to 382 mSv/yr. for the hard-shell module; to stay under the 500 mSv/yr. limit would require that an independent radiation shelter be able to reduce the SPE dosage down to 118 mSv/yr. This requires a radiation protection thickness of at least 350 mm. As the radiation protection layer thickness for GCR increases, the less additional radiation protection for SPE is required.

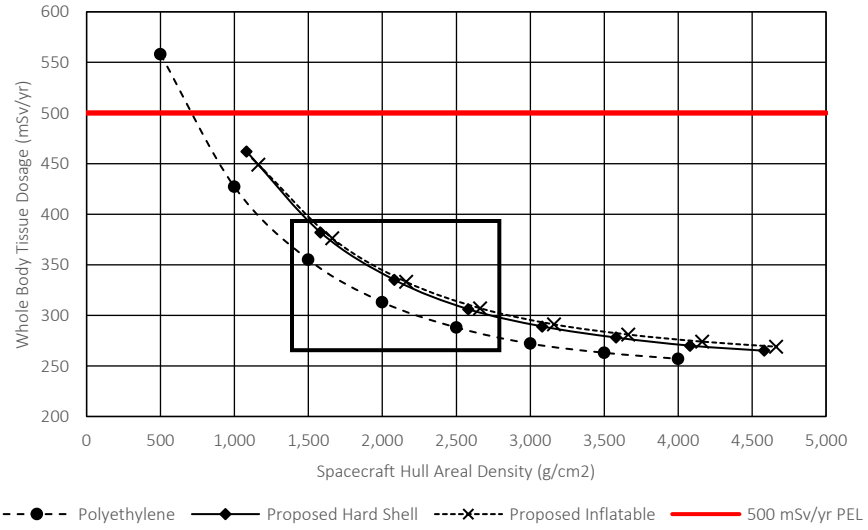

Figure 23: GCR Tissue Dosage for Spacecraft Hull Configurations, as a function of Areal Density

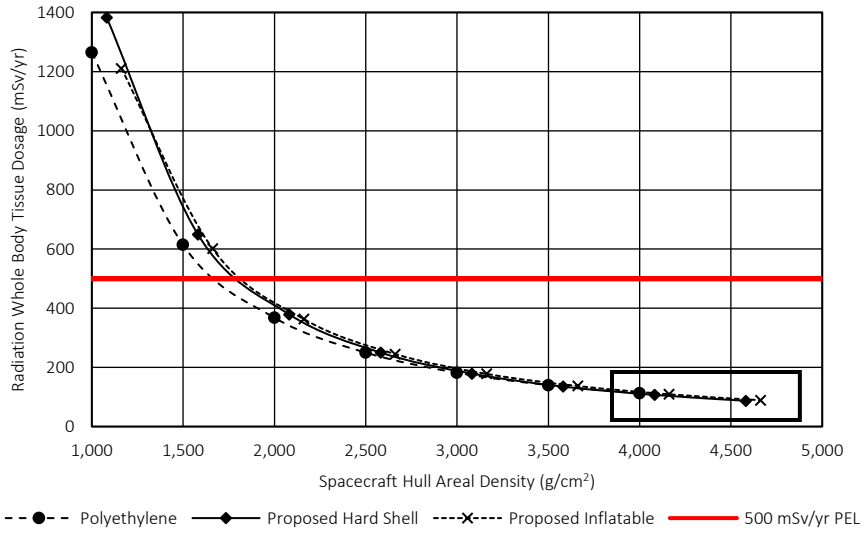

Figure 24: SPE Tissue Dosage for Spacecraft Hull Configurations, as a function of Areal Density

III.3.3 Discussion

It is apparent from figures 1 and 2 that there are performance diminishing returns as the radiation protection layer thickness increases. The GCR data indicates half of the data points fall between 300 – 200 mSv/yr. over an areal density range of ~2,000 g/cm^2. The SPE data performs similar to the GCR data, however the protection from SPE reaches levels below 200 mSv/yr. with the areal densities are at or above 4,000 g/cm^2, something the GCR protection is not able to achieve. This contrast in the data displays the current trade problem, as GCR and SPE protection must balance the risk of crew exposure and the barriers of entry to space. This trade only becomes apparent when planning for long-term, deep space missions as current astronauts and cosmonauts aboard the ISS do not typically spend more than six months in space. According to the baseline data in table 1, the crew's radiation dosages remain below the PEL.

To embark on deep space missions for multiple years does require radiation protection considerations. The trade space for how much radiation protection to provide the crew while remaining within acceptable costs (both for construction and launch) is quite large. This was

the driving factor in simulating a number of radiation protection thicknesses. There is an intent to provide some optimization to the design solution through use of the data. Minimizing mass while keeping below a combined GCR and SPE limit of 500 mSv/yr. requires a number of trades.

The solution suggests tailoring crew exposure to the upper limits of GCR exposure and a radiation protection thickness layer of 100 mm would be adequate (provided the solution incorporates the carbon fiber and Kevlar changes). This minimum GCR protection is only permissible if the crew has access to a radiation shelter for SPE, with at least 350 mm. The combined annual dosage (assuming SPE were to occur similar to the 1989 events) would be 489 mSv/yr. It must be stressed that this is based on simulations with data at 1AU, and prior research suggests this would not be adequate for deep space missions. It is encouraged for further evaluations to be conducted to further characterize the deep space GCR environment and to evaluate/optimize other radiation protection solutions.

If the design solution were to provide the same amount of radiation protection regardless of GCR and SPE preference, a radiation protection layer of 300 mm is required. GCR dosages at 300 mm radiation protection levels for the hard-shell module are 272 mSv/yr. and the SPE dosages are 182 mSv/yr. This approach increases the overall areal density of the hull to ~ 4,000 g/cm^2, whereas the 100 mm GCR and 350 mm SPE approach yields an overall areal density of ~ 2,750 g/cm^2, this assumes equal parts of the spacecraft habitat are dedicated to GCR and SPE protection. The MMOD shielding kept to similar depth distances as per the NASA MMOD guidelines suggest (Christiansen & Lear, 2012), with a depth of ~120 mm. Although not shown, a storm shelter for SPE to keep within the same outer diameter would have to compromise on internal volume to accommodate for the 350 mm radiation protection

layer required to be provided, which would decrease the internal width from 4,000 mm to 3,500 mm.

Figure 26 visualizes a design solution for the hard-shell module with a 100 mm thick radiation protective layer made from polyethylene. The total hull thickness is 291 mm in this design solution and incorporates the radiation protection layer behind the MMOD shielding. Standoffs for the carbon composite were included in the design to give a visual indication to the functions of the layers as well as provide mass properties estimate. A comparison of the design solution's physical properties is compared against the ISS Columbus module in Table 4. The comparison shows that a mass increase of ~5,000 kg is required to achieve sufficient radiation protection from GCR while maintaining a 1AU distance from the sun. The design solution is capable of launching in a SpaceX Falcon Heavy rocket as it meets the payload width requirement is payload to LEO mass requirement of 63,800 kg (SpaceX, 2020). With modification to the external width the design solution could be manufactured for payload fairings of the other major launch vehicles that have a payload to LEO capacity of at least 16,000 kg. This demonstrates the feasibility of launching future spacecraft habitats with quantitatively supported radiation protection design solutions.

Table 11: ISS Columbus Module and Design Solution Comparison

	Width (mm)	Length (mm)	Internal Volume (m^3)	Launch Mass (Empty) (kg)
ISS Columbus Module (European Space Agency (ESA), n.d.)	4,500	6,900	75	10,275
Design Solution Estimate	4,582	6,560	72	15,758

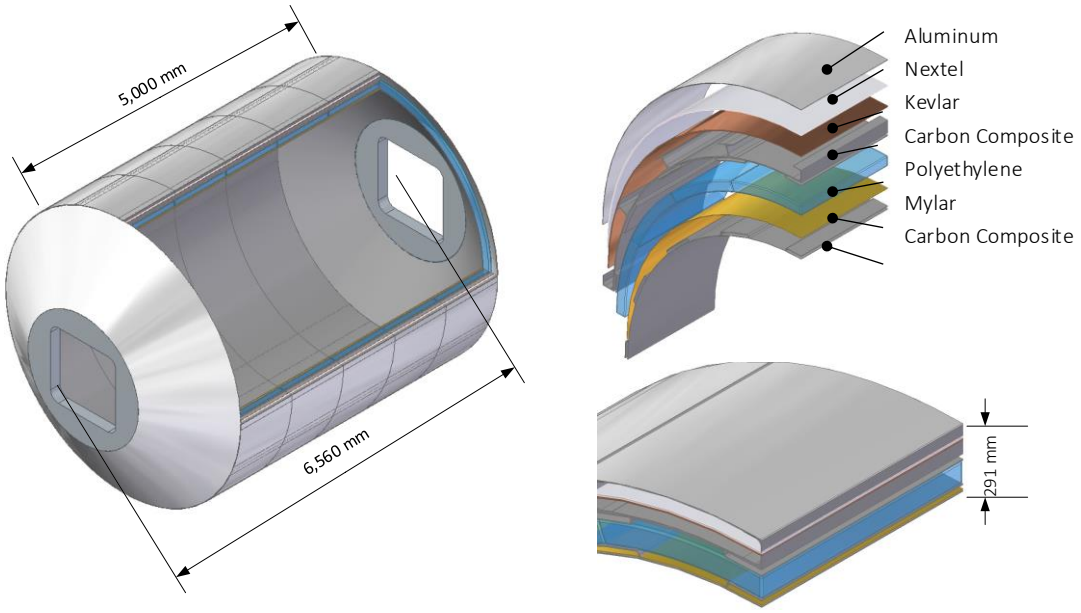

Figure 25: Cross section of a spacecraft hull hard shell design solution

To conclude, spacecraft hull configurations with integrated radiation protective layers were evaluated in OLTARIS to understand the radiation dosage in tissue resulting from these configurations. The simulations demonstrated it is possible to achieve an ALARA level performance limit imposed by NASA of 500 mSv/yr. This is achieved by integrating at least 10cm of polyethylene into a spacecraft hull, for the purposes of operating in a 1AU vicinity. A design solution was formulated based on the simulation results and prior research, resulting in a design solution that implies a feasible launch design into orbit utilizing current launch vehicle technology.

Finally, the next steps to assist future crews embarking on deep space missions are to gather more data on the deep space environment and to perform particle transport experiments at facilities with test articles similar to the design solution shown. Furthermore, perhaps launching a probe with an optimized design solution into deep space while recording the GCR fluences would add to the understanding of radiation protection countermeasures

for deep space travel and allow researchers and engineers to better prepare future crews from the crippling effects of radiation sickness.

IV SPACECRAFT DESIGN SOLUTION

The spacecraft habitat design solution is divided into the exterior and interior sections. The first section describes exterior of the habitat components and how they assemble into the spacecraft. The interior section details how the interior components are assembled by the crew.

IV.1 Spacecraft Exterior Architecture

IV.1.1 Command Module

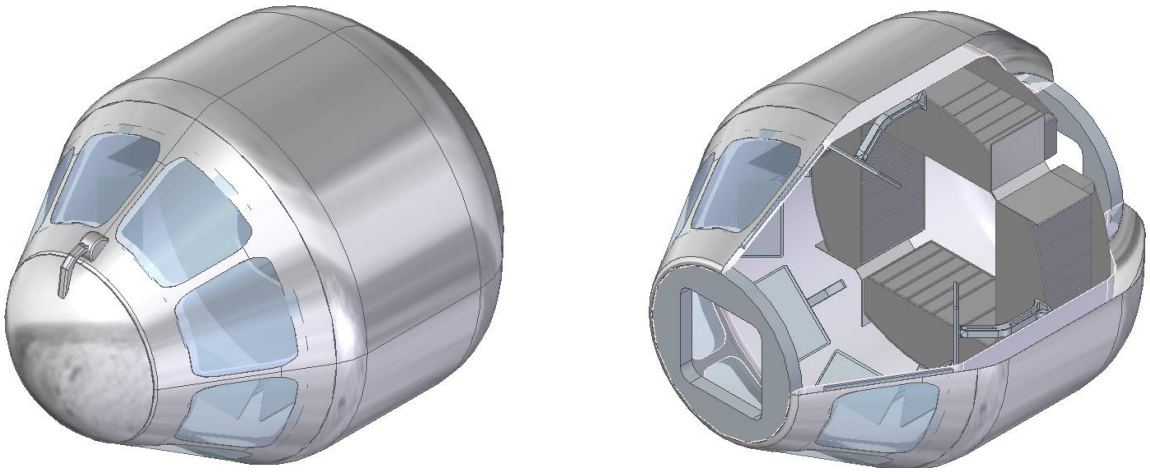

Figure 26: Command Module

The command module has four ISS type racks, which contain the infrastructure to support the subsystems for the spacecraft. Examples of these include small supercomputer clusters, telemetry with internal and external sensors, communications with Earth and spacecraft commanding. The command module contains a standard CBM at the forward nose, and is covered when not in use. A CBM was selected over an International Docking Adapter (IDA) due to its larger physical size, in order to transfer bulk items such as racks and large stowage bags into the main cabin. The current size of the IDA is only 80 cm in diameter, whereas the CBM is 120cm in width. This module is the primary means to dock with another spacecraft. The module is equipped with an array of crew workstations where each station is

similar to that of Mission Control Center (MCC) at JSC. Monitoring of internal systems and subsystems is a 24/7 operation for the workstations as well as the monitoring of solar events, and communicating with Earth, via sending and receiving data.

The windows are made of layers of transparent aluminum and transparent polyethylene, with a UV layer on top and sandwiched with glass layers. Aluminum Oxynitride, also known as transparent aluminum, was simulated in OLTARIS for its radiation transport properties and based on the results, appears to be a candidate for radiation protection while also providing optical transparency properties (Corbin, 1989). Furthermore, it performs well in ballistic testing (McCauley, et al., 2009), therefore it can double as an MMOD shield. The material is quite dense at 3.7 g/cm^3, so it is used sparingly throughout the ship. It is possible to make polyethylene can be made translucent through drawing/extruding methods. When sandwiched with another transparent material such as glass, it achieves about 88-92% transparency for the optical range (Lin, et al., 2019). Polyethylene doubles as a radiation protection material too which the main driver for considering it part of the window assembly. Finally, transparent aluminum was shown to darken in color with a reddish tinge when exposed to ample levels of UV radiation (Du, et al., 2015). It is important not only for the protection of the crew but also to preserve the optical transparency of transparent aluminum that a UV layer be added to the window pane in order to prevent the discolor from occurring.

IV.1.2 Central Module

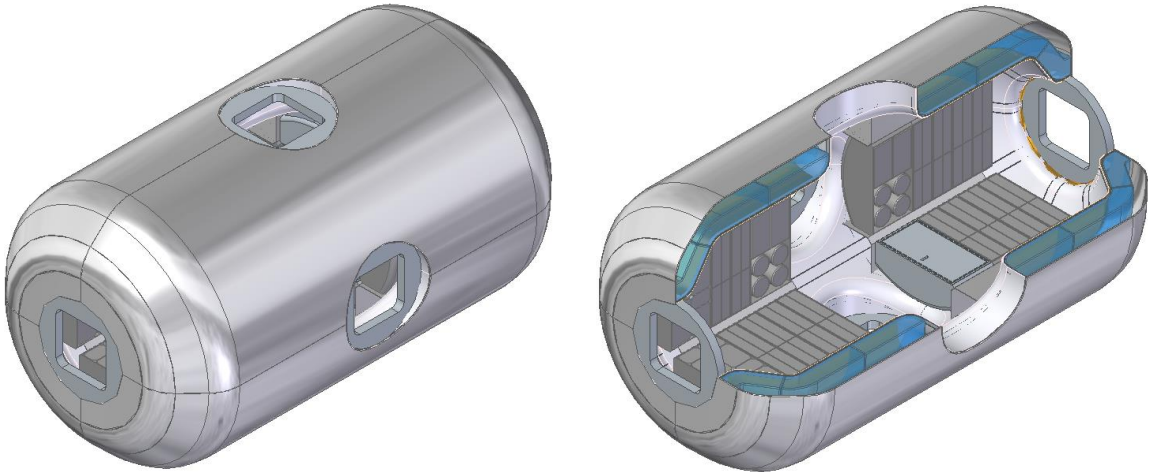

Figure 27: Central Module

The central module is the most important module as it provides the majority of utilities and capabilities for the spacecraft, it is essentially the hub for the spacecraft. According to the design, the central module measures 10 m long and 5.58 m in diameter. The larger diameter is due to the water tanks that surround the pressure vessel. The tanks are required to be 40cm thick and provide both radiation protection from GCR and more specifically SPE, acting as a storm shelter in the event a SPE occurs; as well as water stowage for the crew. The launch vehicles that can launch this module are Blue Origin's New Glenn or SLS Block B. The module contains more ISS type racks, with four racks providing water purification and distribution to the outer modules by interfacing with the surrounding water tanks. Two other racks provide air purification and circulation, both which are centered around the center of the module.

Towards the forward of the module are two racks which act as secondary command and data handling (C&DH) racks in the event of a SPE. There is also a rack dedicated to galley services so the crew working in the command module or science module have quick access to food services if they so wish. In the event of a SPE, the crew will need to make their way to the central module and close the CBM's to the transit modules. These hatches are radiation

hardened with additional mass added to provide adequate protection. The crew will most likely be in the central module on the order of hours to a few days (Cucinotta, et al., 2010), depending on the magnitude of the SPE. The crew may need to sleep, so makeshift sleeping bags should be available to the crew. A rack dedicated to the crew supplies will have all the equipment required to set up a makeshift sleep shelter within the volume of the central Module. Although this is not ideal, SPE's occur infrequently and the probability of lastly on the order of days such that the crew cannot leave the safety of the shelter is small.

The water storage tanks are divided into four sections with each section can hold about 12 metric tons of water, providing a total of 48 tons of water to the crew.

IV.1.3 Science Module

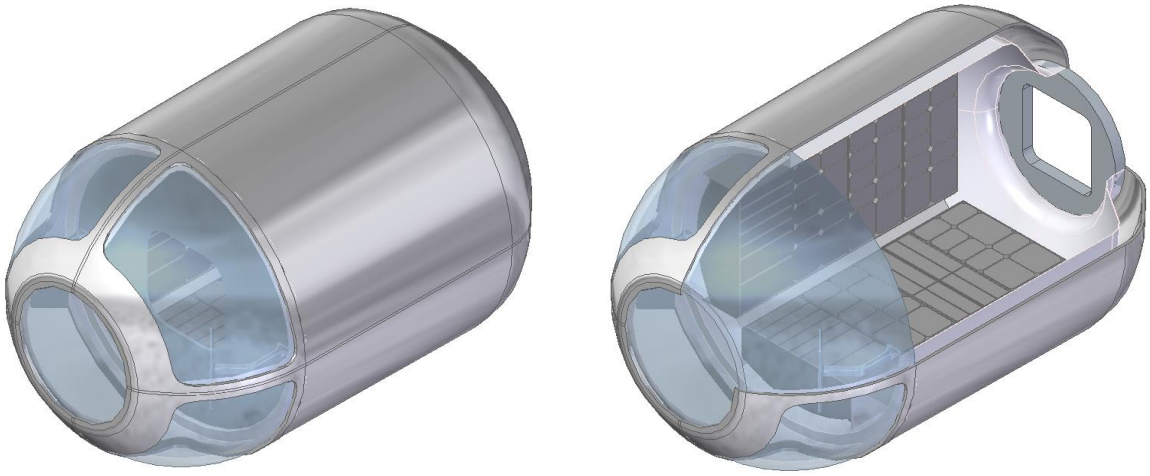

Figure 28: The Science Module

The Science Module is the primary research facility of the spacecraft and no spaceship is without its science facility. It supports 16 ISS type racks, which are all used for science-related work. Some of these racks could be utilized for additional computational power if required. The science module is accompanied with a very large dome, comprised of the same material layered composition as the command module's window panes. This gives the crew an unprecedented view of the stars and any celestial body the spacecraft orbits. The window can

also be utilized as a therapeutic tool for crew who might be struggling with the claustrophobic nature of the spacecraft. It could also provide a view of the spacecrafts rear systems, such as thermal, power and propulsion. This might be useful in the event a component is damaged.

IV.1.4 Transit Module

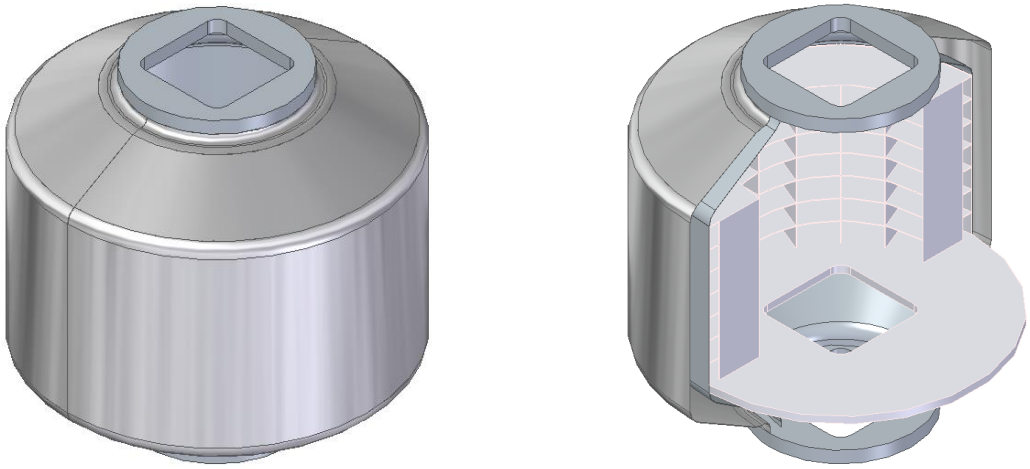

Figure 29: Transit Module

Transit modules are as the name suggests and offer the crew access from the central module to the arc modules, where the crew quarters are located. The transit modules are primarily utilized as spacecraft stowage, providing up to 16 cubic meters of stowage volume. There is a platform on which the crew is able to stand, due to the artificial gravity. Based on SpinCalc website (Hall, SpinCalc, 2018), the platform base which is a distance of 5.82 m from the spacecraft center; at a rotation rate of 6 RPM the amount of g's a crew member would experience is 0.23g. This is slightly more than the g-level at the lunar surface, which is 0.17g's.

The transit module also functions as a utility pass-through module, allowing for the distribution of power, data, water and air to go from the center module to the junction module, and onto the arc modules. The transit module could also serve to facilitate cold stowage and provide crew with access to a frozen food supply extending the shelf life of many food items.

The crew access the transit module by way of ladder and the module is fitted with a standard CBM at each end.

IV.1.5 Junction Module

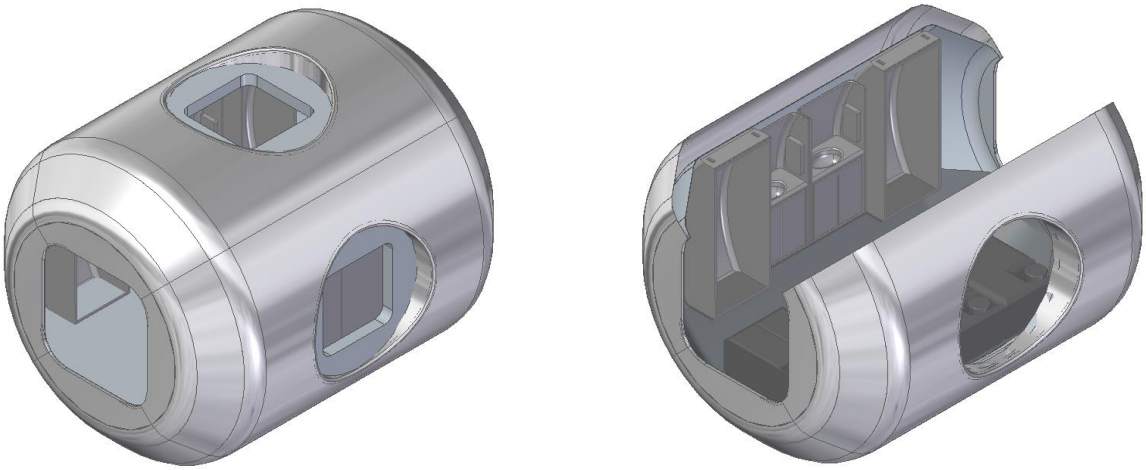

Figure 30: Junction Module

Junction modules connect two inflatable modules together, as well as provide a connection to the transit nodes. Junction nodes provide the water supply for utilities such as toilet, galley and showers to the crew. There is a standard CBM in the top of the module and XL-CBM's on either side of the module, which interfaces with the inflatable modules. Junction modules also have a docking adapter to offload crew and crew supplies without the need to traverse the entire spacecraft through the command module's CBM. This direct access allows for faster and efficient use of robotic and crew ops.

A hard-shell design was adopted over an inflatable due to a number of reasons. Firstly, the complexity of supporting all the systems and the number of interfaces required has not been proven yet in the space environment for inflatables. The inflatable would need to accommodate ports at odd positions, increasing the complexity of incorporating the structure into the fabric layers. Furthermore, due to the size of the spacecraft a small inflatable offers minimal advantages over a small hard-shell module. Perhaps larger spacecraft design could

benefit from inflatable modules acting as junction nodes. Lastly hard-shell modules provide access to mounting equipment and utilities to its structure. Although inflatables could do this by mounting to a core element (as seen in TransHab and Bigelow mockups), this becomes an inefficient use of volume. Due to the nature of the artificial gravity direction, mounting equipment to a specific surface becomes important.

IV.1.6 Arc Module

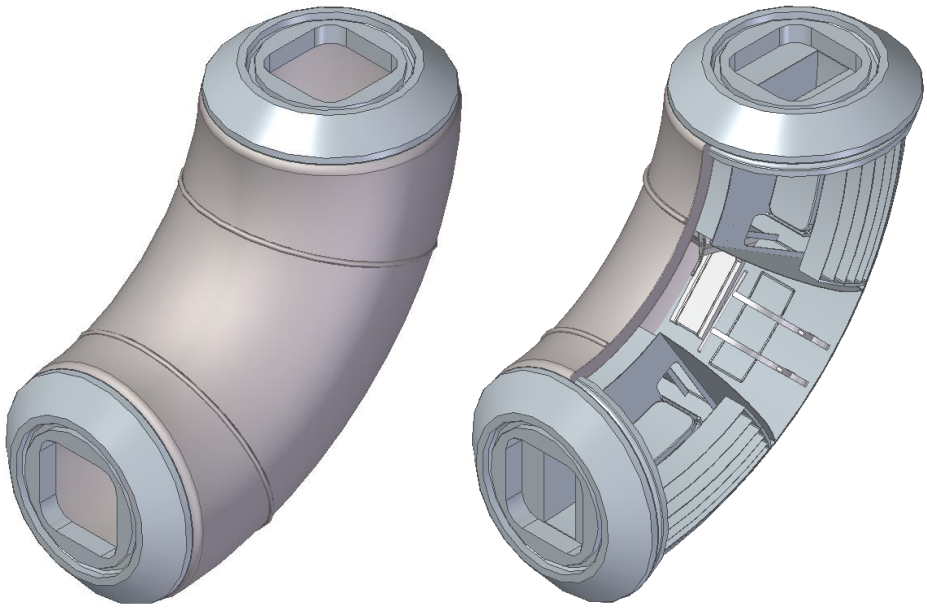

Figure 31: Arc Module

The purpose of a curved inflatable is to fit within a payload fairing of currently utilized launch vehicles. A hard-shell module with a similar curvature profile and size would not fit inside payload fairing of a standard launch vehicle. A different approach (if considering using hard shell modules) would be to divide the modules up into smaller segments. However, this presents more logistical challenges as the number of robotic assembly operations increases as well as the number of launches leading to increased costs and man hours. The arc module inflatable is based on wound inflatable technology (Harris & Kennedy, 2000). Wound inflatables are similar to those used by the US Army, as well as other applications such as

inflatable arches. The inflatable curvature accommodates a curved surface which the crew can stand on. A curved surface is ideal during periods where the spacecraft is in rotation, generating centripetal forces for the crew.

The thickness of the inflatable is ~40cm, which is based on the radiation protection research. This thickness is the minimum to ensure that the crew are able to live in the inflatable during GCR periods and still be below the 500 mSv/yr. limit if a SPE occurs. According to the transhab paper that shows the layers (Badhwar, Huff, Wilkins, & Thibeault, 2001), there are many layers that make up the inflatable. The only change proposed is the addition of polyethylene blankets to increase the radiation protection effectiveness.

The berthing interfaces at each end of the inflatable are based off the CBM utilized on the ISS. However, due to the nature of the artificial gravity environment, these interfaces have been enlarged to accommodate for large equipment items and to ensure the crew do not have to use large bending motions walk through the bulkhead while in an artificial gravity state. These are hence named Extra-Large Common Berthing Mechanisms (XL-CBM). Finally, the packing configuration for this module, due to its small size could possibly be packed with minimal creases and be launched on most current launch vehicles.

Figure 32: Arc module packing configuration Falcon 9 example

IV.1.7 External Elements Construction Concept of Operations

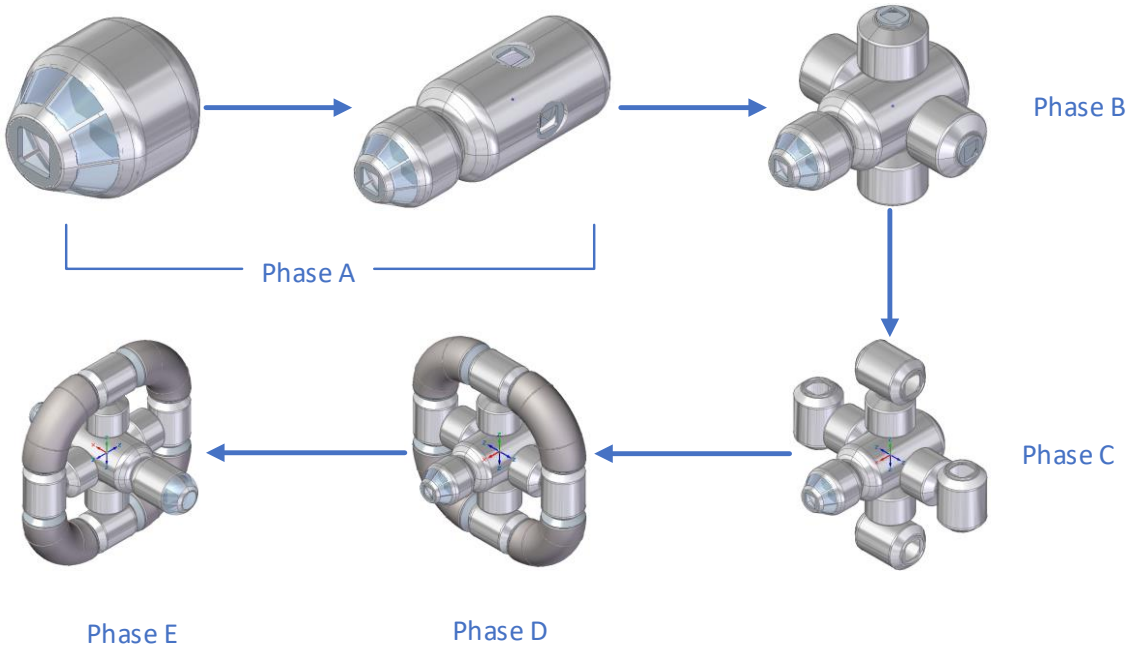

Figure 33: Phases of Construction

The spacecraft habitat is assumed to be built at an assembly space station, with robotic operation capabilities. The assembly sequence is organized into phases. Phase A: The command module is the first module to dock/berth with the space station, followed by the central module, which will be berthed to the aft of the command module. Subsequent cargo missions to provide the spacecraft's water will follow (not shown). Also a full systems check and diagnostic is performed before any further modules arrive to ensure the spacecraft is able to support these modules. One standard launch and one heavy lift launch is required to deliver these modules to LEO.

Phase B: The four transit modules will arrive once the phase A modules are cleared for additional support, they will be berthed using robotic ops. The transit nodes may launch with food supplies already stowed if launch mass allows. Two minimum launches are required for delivery to LEO (if a payload fairing can accommodate two of them) but possibly up to four.

Phase C: Each junction module will be launched with a section of crew flooring, walls, ceiling and subsection infrastructure. These modules will be berthed robotically and will require four standard launches.

Phase D: Each arc module will be launched in a packed/folded configuration. The robotic operations will berth one end to one junction node and then to the other. The flexibility of the fabric should allow for relative ease of installation. Once all four modules are in place, the entire cabin will be pressurized. Then the crew will begin to assemble the interior sections of the habitat.

Phase E: The science node is installed and additional exterior systems are also installed at this time.

The coordinate system of the spacecraft is set to a local coordinate system with the center at the center of the central module. Forward is along the positive X-Axis and Aft is along the negative X-Axis. Port is along the positive Y-Axis and Starboard is along the negative Y-Axis. Zenith is along the positive Z-Axis and Nadir is along the negative Z-Axis. The YZ plane intersect the central, transit, junction and arc modules. Positive rotation is counter clockwise and is about the X-Axis.

Each module in the spacecraft is considered a node, with the following naming conventtion applied. The letter designation for each module is N-X0, with X a letter placeholder and 0 as a numerical placeholder. The modules along the X-Axis are designed with C1 – 3, the C designation communicating the modules are on the center axis of rotation. The N designation communicates the modules are nodes by which the crew can access. The letters Z, P, N, S and A are Zenith, Port, Nadir, Starboard and Arc.

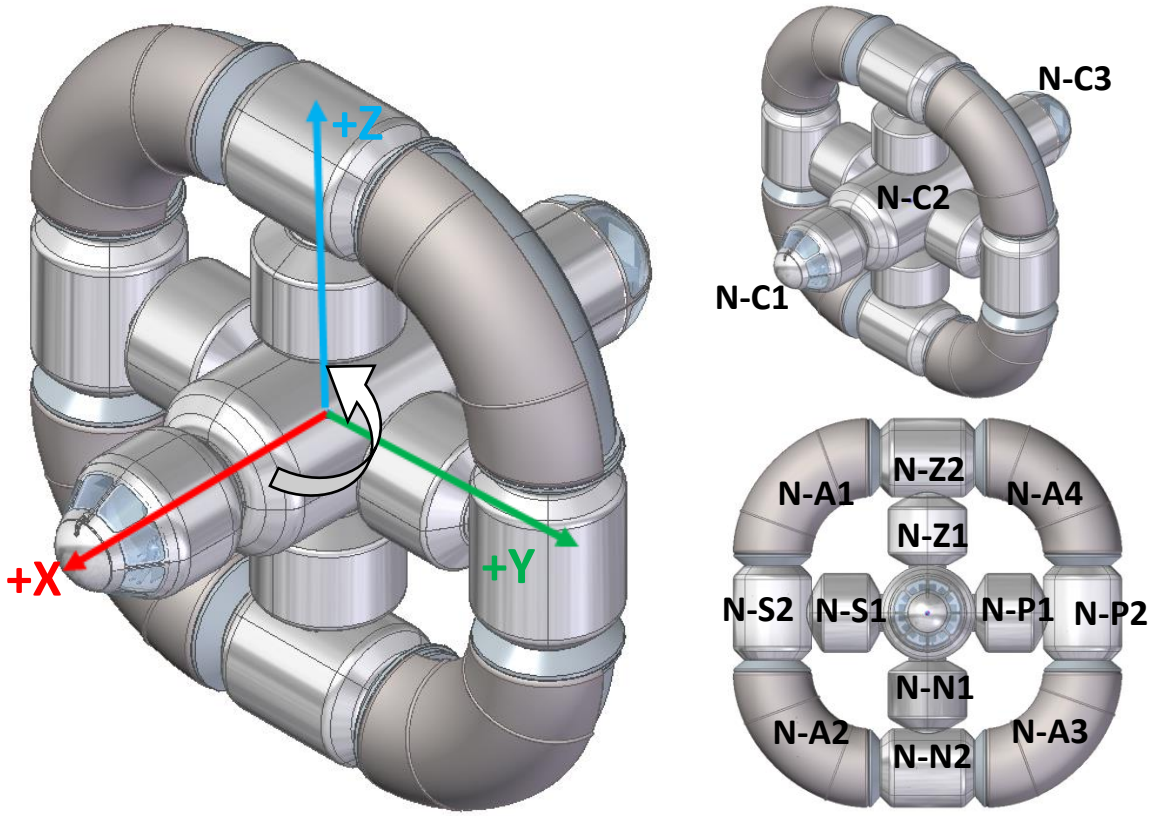

Figure 34: Spacecraft Coordinate system and Node Naming Conventions (isometric view looking aft-starboard-nadir and looking aft)

IV.2 Spacecraft Interior Architecture

IV.2.1 Arc Module Outfitting

The outfitting of the arc module occurs once there is pressurized atmosphere within the module and the crew are able to enter. The junction modules contain the equipment to begin the outfitting process, which are the stowage frame, the platform, the outer walls, the inner walls and the utility roof. All the equipment requires assembly for it to be packed in the junction module. Additional items such as shelving, beds and frames and crew configuration preferences will require additional cargo missions to facilitate the completion of the outfitting process. Once this process is complete however, it is assumed that minimal changes will need

to be made for each crew rotation. Figure 35 shows the packing configuration for the parts involved, ready for launch:

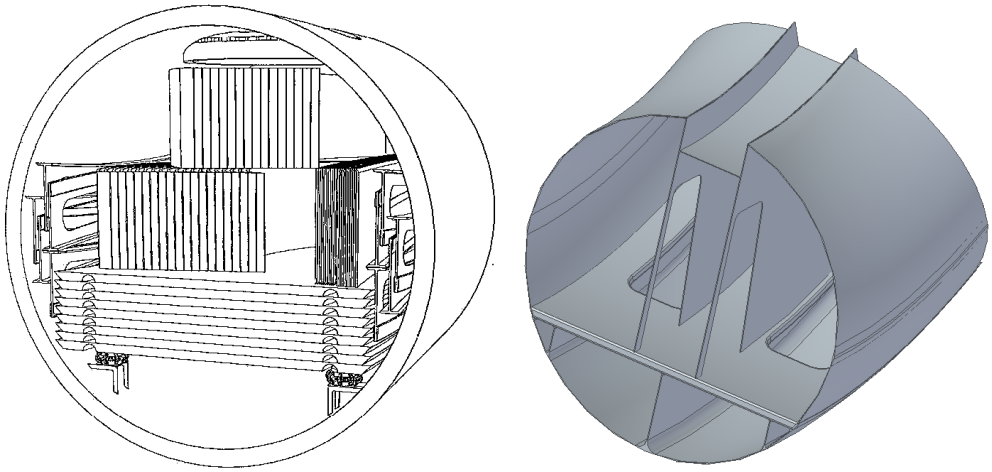

Figure 35: Component packing configuration (left) and assembled configuration(right)

The outfitting of the internal elements is organized into phases. Each section of the arc module will have all the structural elements packed into an adjacent junction module. The internal elements to be packed include the floors, walls and utility roofs. The elements are required to be manufactured in segments in order to fit through the hatches between the arc and junction modules and assembled by the crew once on orbit. The first phase is the assembly of the sub-floor segments, where they will house utility lines for power and data as well as airflow ventilation. The sub-floor segments also provide flexible crew or mission stowage options.

The second phase is the placement of the floor panels, which provide a platform to mount the walls and equipment. The third phase is the placement of the walls and utility roofs. The outside walls require support from the internal walls and the roofs provide a path for lights and power/data lines to be mounted. Airflow can also be distributed through the

roofline by the addition of ducting. Once these structural elements are mounted and in place, the furbishing of the interior can commence in the final phase.

The final phase is the furbishing of each segment that will be utilized for a variety of tasks such as housing the crew, providing exercise facilities, accommodating for a recreation space and providing a workspace. These elements are to be sent up via additional cargo vehicles. The assembly station the spacecraft docks to will provide additional stowage space for the refurbishment and reconfiguration process. The station could store additional items that support a variety of mission types.

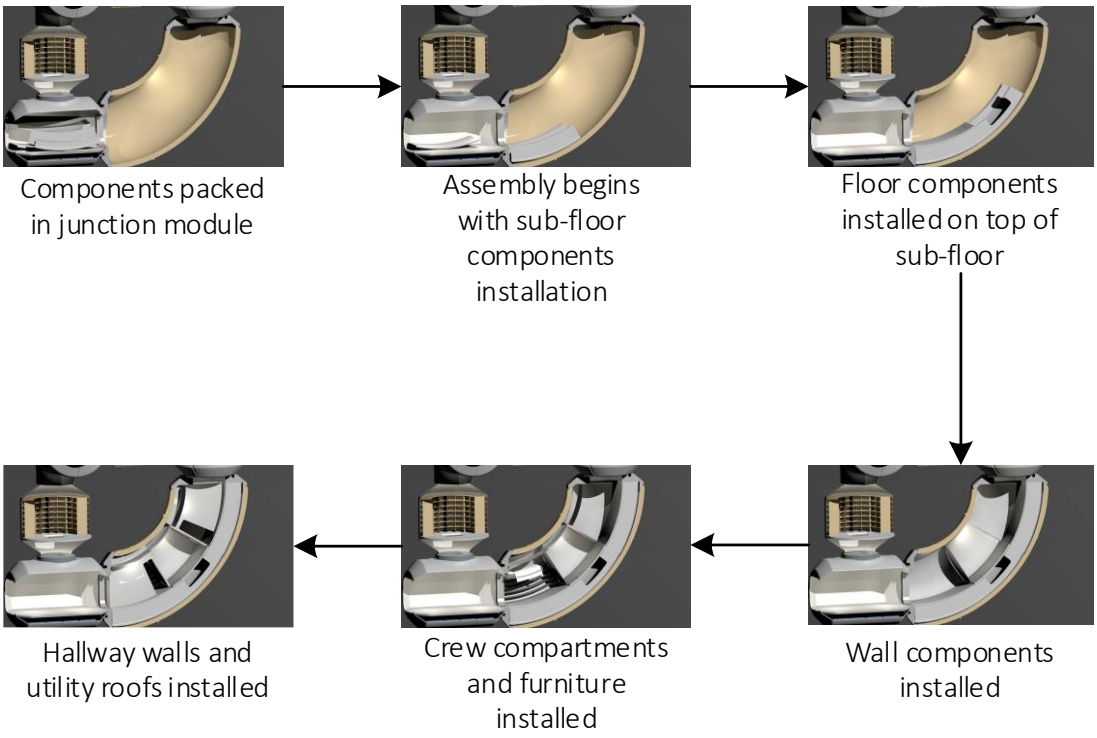

Figure 36: Assembly stages of the interior outfitting operations

Figure 37 provides views of the configuration for one set of crew quarters. The platform contains large access cutouts to the stowage area. This allows for flexibility in crew member preference, whether to turn the space into a desk space or use more of it for stowage. Although not shown there will be adjustable floor covers to give the crew the flexibility to

cater their crew quarters to the aesthetic and function of their choice. The beds shown are twin sized mattresses and are in an elevated position to open up access to the stowage area below. The bed frame is connected to hinges on the wall and the shelving as shown in the Figure 37 below. The bed frame position is adjustable based on crew preference.

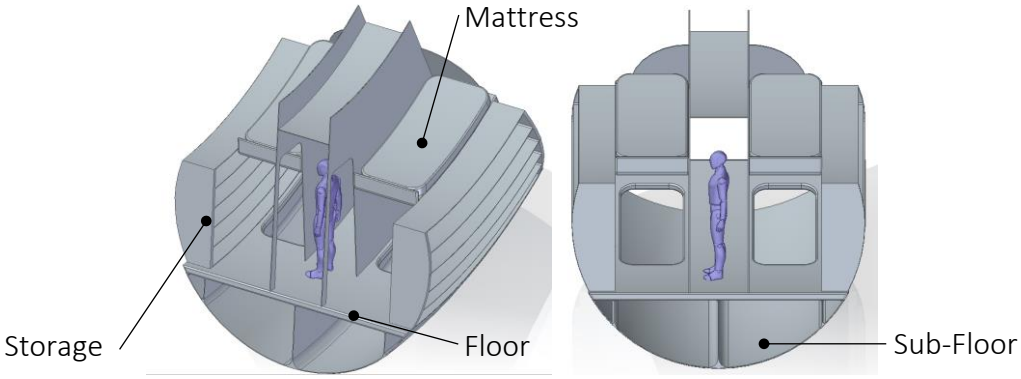

Figure 37: Views of crew quarters

There are two gyms in this current spacecraft configuration, each of them is positioned between the crew quarter segments. There is adequate surface area to place equipment such as a treadmill or exercise bike as well as equipment to support resistance training equipment. The arc length of the gym segment is slightly shorter than the crew quarters, since the crew will spend more time in their quarters than the gym, it was important to optimize the living space to suit this need.

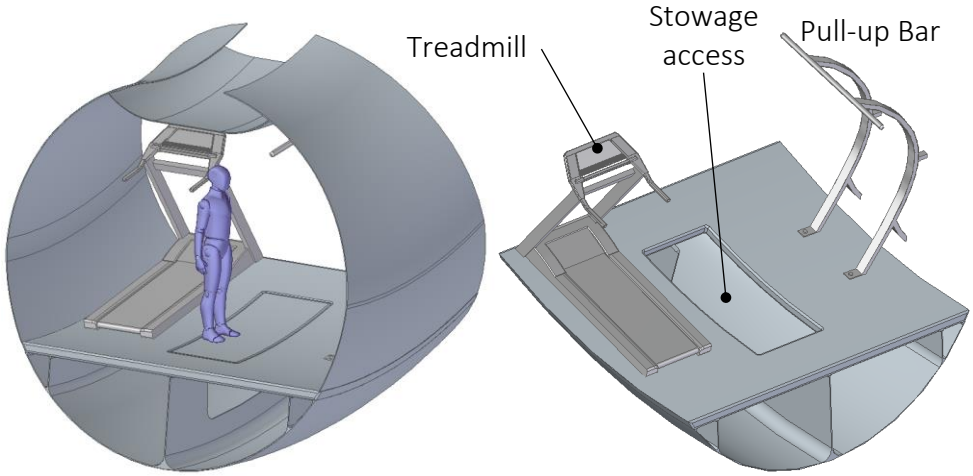

Figure 38: Gym segment

The multi-purpose room is an area that can be utilized for a variety of functions. Currently its functions are thought to have functional workspaces for the crew as well as recreational spaces. The multi-purpose room is made from a crew quarter segment and gym segment. Figure 39 shows the multi-purpose room and some of its potential uses and configurations:

Figure 39: Multi-purpose room potential configuration

The airflow is circulated through the cabin by fan circulation, there are racks in the central and junction modules which supply the necessary ECLSS functions for air filtering and scrubbing CO2. The airflow begins in the central module and flows through two of the transit modules to the junction module where the ECLSS cleans it before pushing is through each arc module. The other two junction and transit modules are utilized to filter the air again and push it back to the central module. The water distribution is limited to the central, transit and junction modules. The transit module acts as a pass-through for the water, where at the junction module the water is utilized by the crew for daily use such as toilets, showers and food/liquid consumption. The central module will also have a small food processor as well as

a toilet for crew who are working in the micro-g environment. Figure 39 describes the airflow and water distribution, the green/grey arrows describe clean air (green) circulating around the cabin and getting dirty (grey) before getting scrubbed by the ECLSS system.

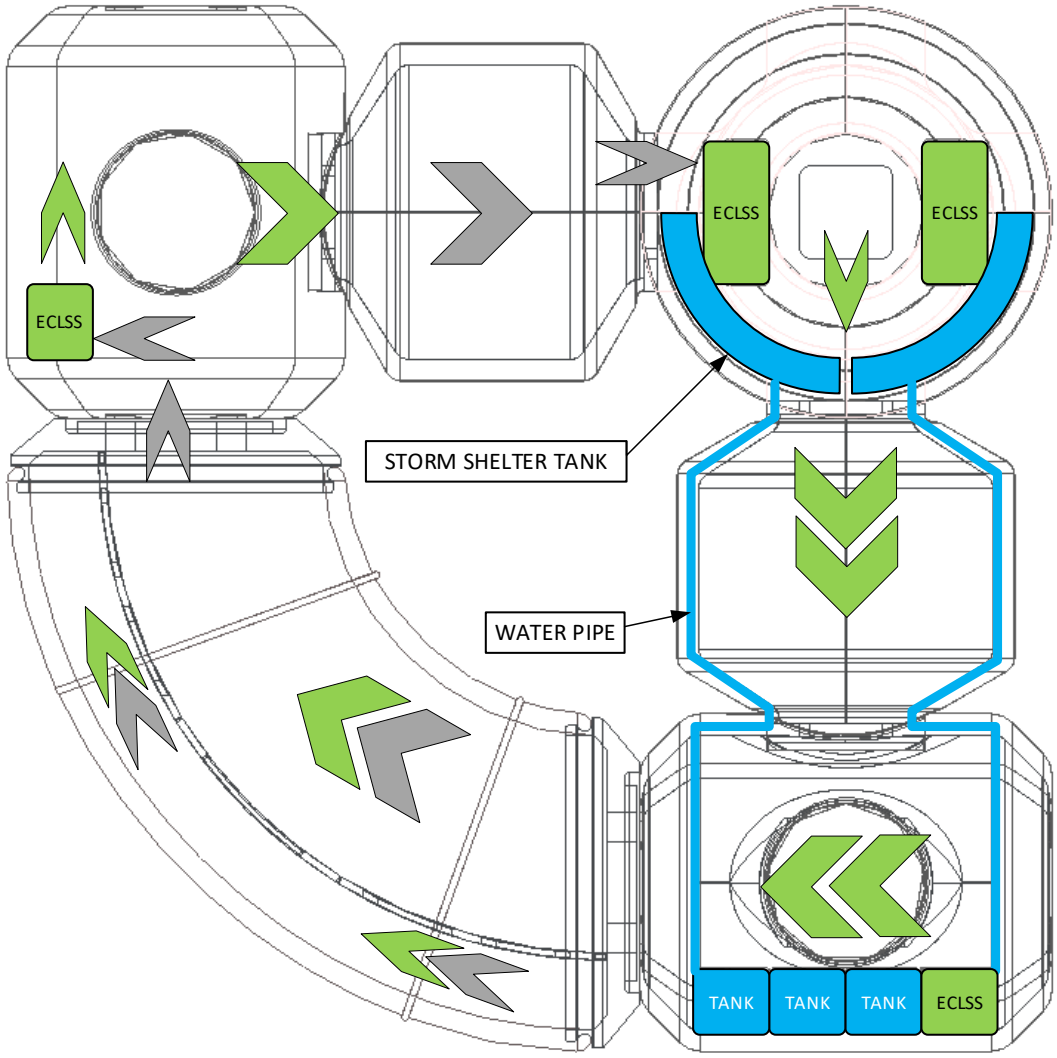

Figure 40: Air and Water distribution

IV.2.2 Configuration Management

The cabin can be configured in various ways to meet the requirements for each mission. Once the primary structural elements have been installed, the secondary elements such as desk, chairs, partitions, etc. can be repositioned or removed to allow different

configurations. An example of two missions requiring different configurations is a Venus exploration mission with a short mission duration; the crew are expected to perform many science-related tasks during the mission and due to this, the rotating habitat is configured with additional science workspaces. Contrast the Venus mission with a Mars mission which might require the crew to orbit the planet for six months, increasing the mission time over Venus by almost a year. Crew comforts are likely to take priority over science-related tasks due to the longer mission duration, resulting in an increase in allocated volume for crew related activities (Whitmire, et al., 2015).

This could again be vastly different from a lunar tourism configuration, where the spacecraft does frequent cargo missions to the Moon and takes on a compliment of space tourists who pay to experience space travel. The rotating habitat for this configuration would increase the number of sleeping quarters, perhaps adopting smaller accommodations for the tourists and providing an activity space for them. An additional configuration criterion is ensuring the mass for each section is balanced so as to not introduce precession effects from the spacecraft rotation. The flexibility to design the cabin to fit the mission is a critical design feature to ensure the longevity of future spacecraft.

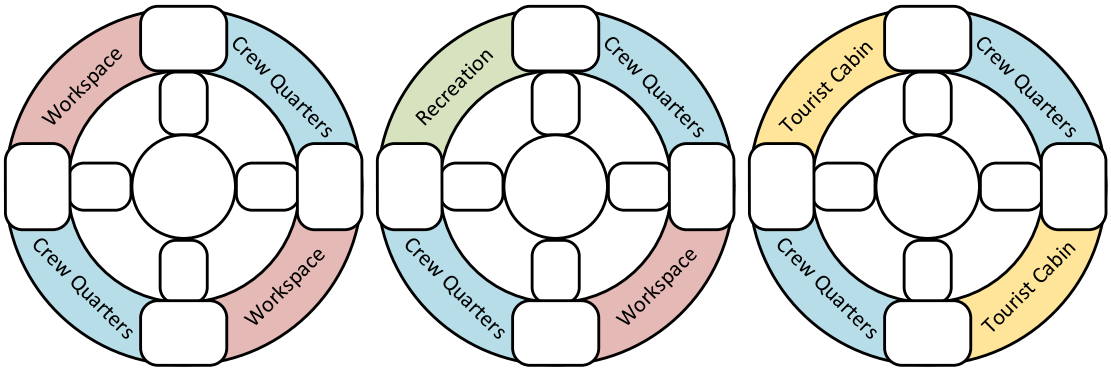

Figure 41: Venus Example Configuration (left), Mars Example Configuration (middle), Lunar Tourism Configuration (right)

The following figures provide renders of the spacecraft habitat with an example configuration. These renders provide images of the command module, center module, crew ablutions in a junction module, crew galley in a junction module and the science module.

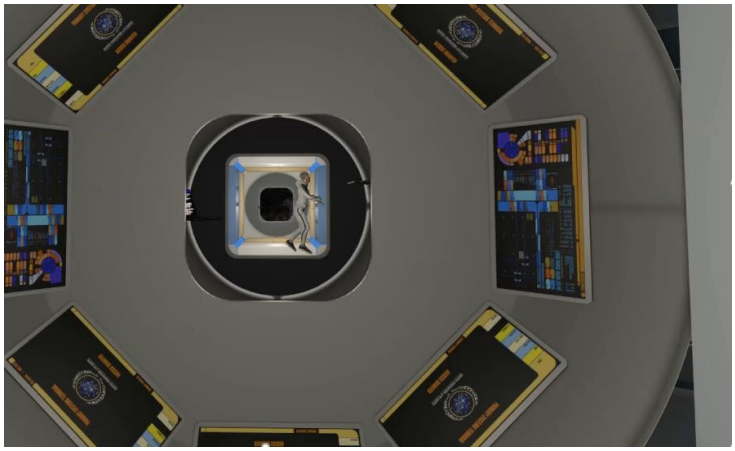

Figure 42: Command module operations stations view, looking aft

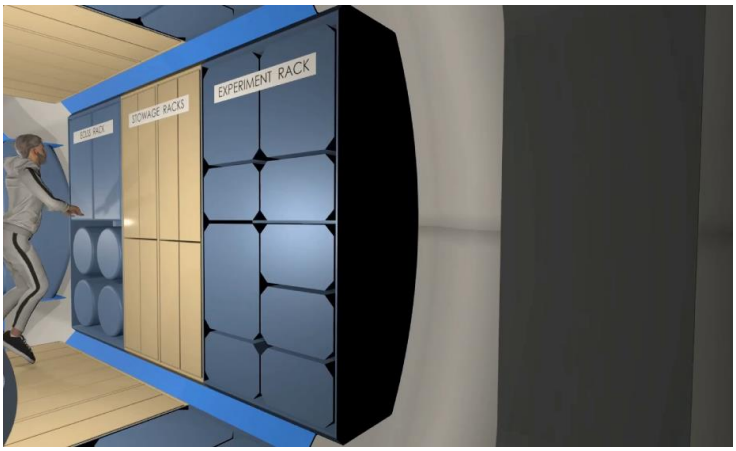

Figure 43: Center module rack view

Figure 44: Crew ablutions with shower, hand basins and washer/dryer unit

Figure 45: Crew galley with kitchenette rack, stowage and refrigerator units

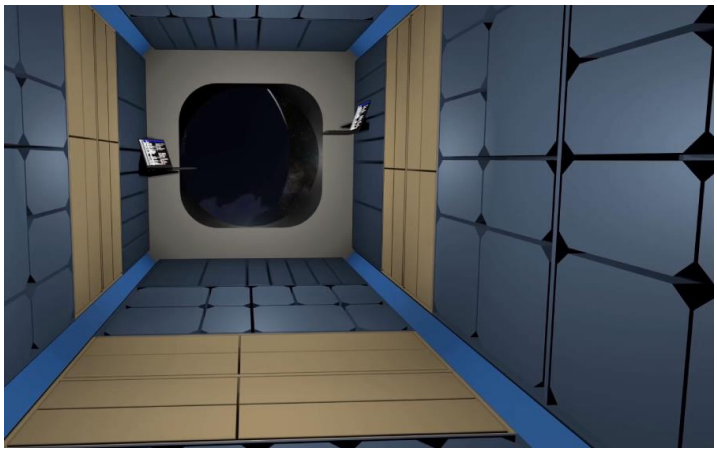

Figure 46: Science module with experiment racks, stowage and laptops

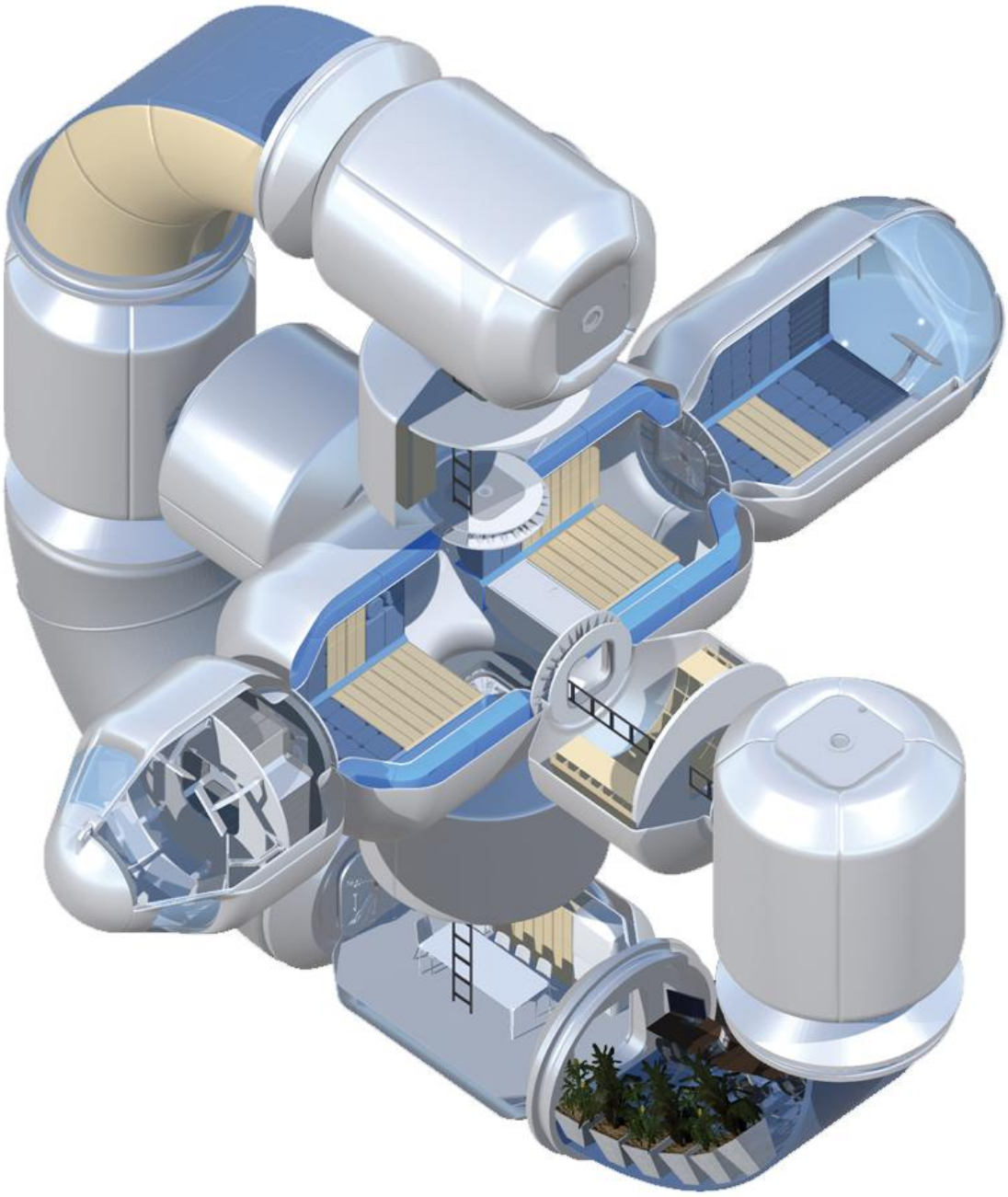

Figure 47: Spaceship habitat cutaway view - full page render

V CONCLUSION

It was stated at the beginning of this thesis that humanity is close to starting a new chapter in the story of the human space fairing civilization. This thesis sort to reconcile two major issues that cause humans harm in the space environment: micro-gravity and space radiation. Through an analysis of habitat geometries, it was determined a torus structure was the most suitable geometry for an artificial gravity enclosure. Understanding the Coriolis forces allowed for the practical placement of crew quarters, facilities and spacecraft habitat concept of operations. An investigation into internal rotating platforms produced a feasible curved platform design which was integrated into the final spacecraft habitat design.

Materials research guided the analysis of spacecraft hulls for their radiation transport properties. Radiation transport simulations further added verifiable results to the hypothesis that the addition of feasible sized radiation shielding layers could be launched into orbit. The research produced spacecraft hull configuration design solutions that met the NASA permissible energy levels for astronauts.

The research and design solutions were then molded into a spacecraft habitat concept design which meets the requirements initially set out in the beginning of this thesis. The spacecraft habitat concept incorporates a curved platform geometry to accommodate the crew during artificial gravity operations. The habitat provides enough stowage for a three-year mission and contains the functionality to perform science, similar to what is performed currently on the ISS. The assembly of the spacecraft is feasible due to the design compatibility of each spacecraft module to the current fleet of launch vehicles.

The intent of this thesis was to produce a feasible spacecraft habitat design with construction capabilities utilizing technologies available. It is the hope of this author that this thesis allows the space community to come one step closer to writing that next chapter.

REFERENCES

Arianespace. (2016, October). *Ariane5_Users-Manual_October2016*. Retrieved from http://www.arianespace.com/wp-content/uploads/2011/07/Ariane5_Users-Manual_October2016.pdf

Badhwar, G. D., Huff, H., Wilkins, R., & Thibeault, S. (2001). Comparison of graphite, aluminum, and TransHab shielding material characteristics in a high-energy neutron field. *Radiation Measurements, 35*, 545-549.

Bahadori, A., Semones, E., Ewert, M., Broyan, J., & Walker, S. (2017). Measuring space radiation shielding effectiveness. *EPJ Web of Conferences 153*.

Barthel, J., & Sarigul-Klijn, N. (2017). Adaptive, Readily Morphing, Optimized Radiation Shielding for Transit Habitats: Flyby Mars Mission. *Journal of Spacecraft and Rockets*.

Bigelow Aerospace. (2011, May 25). Retrieved from http://images.spaceref.com/news/2011/bigelow.chrtz.isdc.pdf

Bigelow Aerospace. (2018). *B330*. Retrieved from Bigelow Aerospace: https://bigelowaerospace.com/pages/b330/

Birnbaum, S. (1999). *Force On A Runner's Foot*. Retrieved from hypertextbook.com: https://hypertextbook.com/facts/1999/SaraBirnbaum.shtml

Biron, M. (2017). 5 - Biobricks: The Breakthrough of Drop-In Solutions. In *Industrial Applications of Renewable Plastics* (pp. 155-369). Elsevier Ltd.

Blue Origin. (2018, October). *New Glenn Payload User's Guide*. Retrieved from Blue Origin: https://www.blueorigin.com/new-glenn/new-glenn-payload-users-guide

Boezio, M., & Mocchiutti, E. (2012). Chemical composition of galactic cosmic rays with space experiments. *Astroparticle Physics*, 95-108.

Cane, H. V., Richardson, I. G., & von Rosenvinge, T. T. (2010). A study of solar energetic particle events of 1997-2006: Their composition and associations. *Journal of Geophysical Research*.

Christiansen, E., & Lear, D. (2012, February 24). *Micrometeoroid and Orbital Debris Environment and Hypervelocity Shields*. Retrieved April 5, 2020, from https://ntrs.nasa.gov/archive/nasa/casi.ntrs.nasa.gov/20120002584.pdf

Corbin, N. D. (1989). Aluminum Oxynitride Spinel: A Review. *Journal of the European Ceramic Society*, 143-154.

Cucinotta, F. A., Hu, S., Schwadron, N. A., Kozarev, K., Townsend, L. W., & Kim, M.-H. Y. (2010). Space radiation risk limits and Earth-Moon-Mars environmental models. *Space Weather*.

Dodson, B. (2013, August 22). *Beyond the hype of Hyperloop: An analysis of Elon Musk's proposed transit system*. Retrieved from New Atlas: https://newatlas.com/hyperloop-musk-analysis/28672/

Du, X., Yao, S., Jin, X., Chen, H., Li, W., & Liang, B. (2015). Radiation damage and luminescence properties of gamma aluminum oxynitride transparent ceramic. *Journal of Physics D: Applied Physics*.

Durante, M., & Cucinotta, F. A. (2011). Physical basis of radiation protection in space travel. *Reviews of Modern Physics*, 1245-1281.

European Space Agency (ESA). (n.d.). *ISS: Columbus Module*. Retrieved April 2020, 1, from https://earth.esa.int/web/eoportal/satellite-missions/i/iss-columbus

Finckenor, M. M., & Dooling, D. (1999, July 9). *Multilayer Insulation Material Guidelines*. Retrieved April 8, 2020, from https://ntrs.nasa.gov/archive/nasa/casi.ntrs.nasa.gov/19990047691.pdf

Hall, T. W. (2016). Artificial Gravity in Theory and Practice. *46th International Conference on Environmental Systems* (pp. 194-214). Vienna: International Conference on Environmental Systems.

Hall, T. W. (2018, September 9). *SpinCalc*. Retrieved from Artificial Gravity: https://www.artificial-gravity.com/sw/SpinCalc/

Harris, P., & Kennedy, K. (2000). Wound Construction of Inflatable Space Structures. *SPACE 2000* (pp. 417-423). Albuquerque, New Mexico: American Society of Civil Engineers (ASCE).

Henderson, E. M., & Holderman, M. L. (2011, July 7). *Technology Applications that Support Space Exploration*. Retrieved from NASA Technical Reports Server (NTRS): https://ntrs.nasa.gov/archive/nasa/casi.ntrs.nasa.gov/20110013138.pdf

Holderman, M. L. (2011, January 26). *Nautilus-X. Multi-Mission Space Exploration Vehicle*. Retrieved from Web Archive University of Texas: https://web.archive.org/web/20110304044259/http://spirit.as.utexas.edu/~fiso/telecon/Holderman-Henderson_1-26-11/Holderman_1-26-11.ppt

Jevtovic, P. (2015). Electrodynamic Gravity Generator. *AIAA SPACE Conference*. Pasadena, CA: AIAA.

Joosten, K. B. (2007, August 1). *Preliminary Assessment of Artificial Gravity Impacts to Deep-Space Vehicle Design*. Retrieved from NASA Technical Reports Server (NTRS): https://ntrs.nasa.gov/archive/nasa/casi.ntrs.nasa.gov/20070023306.pdf

Kaul, R. K., Barghouty, A. F., & Danche, H. M. (2004). Space Radiation Transport Properties of Polyethylene-Based Composites. *Annals New York Academy of Sciences*, pp. 138-149.

Lin, Yunyin; Patel, Ruhi; Cao, Jun; Tu, Wei; Zhang, Han; Bilotti, Emiliano; Bastiaansen, Cees W.M; Peijs, Ton. (2019). Glass-like transparent high strength polyethylene films by tuning drawing temperature. *Polymer*, 180-191.

McCauley, J. W., Patel, P., Chen, M., Gary, G., Strassburger, E., Paliwal, B., . . . Dandekar, D. P. (2009). AlON: A brief history of its emergence and evolution. *Journal of the European Ceramic Society*, 223-236.

Minster, G., Chang, A., Inouye, J. B., Narayanan, S., Carter, A., Tong, J., & Barnhart, D. (2018). Hyperion: Artificial Gravity Reusable Crewed Deep Space Transport. *69th Internation Astronautical Congress (IAC)*. Bremen, Germany: International Astronautical Federation (IAF).

Mrigakshi, A. I., Matthia, D., Berger, T., Reitz, G., & Wimmer-Schweingruber, R. F. (2013). Estimation of Galactic Cosmic Ray exposure inside and outside the Earth's magnetosphere during the recent solar minimum between solar cycles 23 and 24. *Advances in Space Research*, 979-987.

Narici, L., Casolino, M., Di Fino, L., Larosa, M., Picozza, P., Rizzo, A., & Zaconte, V. (2017). Performances of Kelvar and Polyethylene as radiation shielding on-board the International Space Station in high latitude radiation environment. *Nature*.

NASA. (2016, December 22). *Trajectory Search*. Retrieved from NASA Ames Research Center Trajectory Browser: https://trajbrowser.arc.nasa.gov/traj_browser.php

NASA. (2018, December 19). *Space Launch System (SLS) Mission Planner's Guide*. Retrieved from NASA Technical Reports Server: https://ntrs.nasa.gov/search.jsp?R=20170005323

National Aeronautics and Space Administration (NASA). (2017, August 2017). *Technology Readiness Level*. Retrieved from NASA:

https://www.nasa.gov/directorates/heo/scan/engineering/technology/txt_accordion1.html

National Aeronautics and Space Administration (NASA). (2019, July 31). *HRR - Risk - Risk of Radiation Carcinogenesis*. Retrieved April 12, 2020, from https://humanresearchroadmap.nasa.gov/Risks/risk.aspx?i=96

National Aeronautics and Space Administration (NASA). (2019). *Human Research Program Integrated Research Plan.* Houston, TX: Lyndon B. Johnson Space Center.

Sazali, M. A., Rashid, N. K., & Hamzah, K. (2018). A review on multilayer radiation shielding. *International Nuclear Science, Technology and Engineering 2018*. IOP Conf. Series: Materials Science and Engineering 555.

Singleterry, Robert C; Blattnig, Steve R; Clowdsley, Martha S; Qualls, Garry D; Sandridge, Christopher A; Simonsen, Lisa C; Norbury, John W; Slaba, Tony C; Walker, Steven A; Badavi, Francis F; Spangler, Jan L; Aumann, Aric R; Zapp, E. Neal; Rutledge, Robert D; Lee, Kerry T; Norman, Ryan B. (2010). *OLTARIS: On-Line Tool for the Assessment of Radiation in Space.* NASA.

SpaceX. (2019, January). *Falcon User's Guide.* Retrieved from https://www.spacex.com/sites/spacex/files/falcon_users_guide_10_2019.pdf

SpaceX. (2020). *Falcon Heavy | SpaceX*. (SpaceX) Retrieved May 2, 2020, from https://www.spacex.com/falcon-heavy

Todd, P. (2003, June). Space Radiation Health: A Brief Primer. *Gravitational and Space Biology Bulletin 16*, pp. 1-4.

United Launch Alliance. (2010). *atlasvusersguide2010.* Retrieved from https://www.ulalaunch.com/docs/default-source/rockets/atlasvusersguide2010.pdf

United Launch Alliance. (2013, June). *Delta IV Launch Services User's Guide.* Retrieved from https://www.ulalaunch.com/docs/default-source/rockets/delta-iv-user's-guide.pdf

Vibro/Dynamics LLC. (2018). *Socitec wire rope isolators and cable mounts*. Retrieved from Vibro/Dynamics vibration isolators, machine mounts, cable mounts, wire rope isolators: http://www.vibrodynamics.com/usa/wire_rope.html

Vibrostop. (2018). *AVAUD - Wire rope isolator*. Retrieved from https://www.vibrostop.it/en/product/wire-rope-isolators/avaud/

Whitmire, A., Leveton, L., Broughton, H., Basner, M., Kearney, A., Ikuma, L., & Morris, M. (2015). *Minimum acceptable net habitable volume for long-duration exploration missions.* Houston, Texas: NASA.

Wu, Zhengxin; Ma, Yugang; Lu, Jinbin; Sun, Huibin; Liu, Guoqing; Zhao, Haige; Wang, Yin; Hu, Yanqi. (2019). Comparison of the Radiation Shielding Properties of Wall Materials for the Manned Spacecraft for Future China Space Exploration Missions. *Journal of the Korean Physical Society*, 666-671.

Zipay, J. J. (2019, January 7). *Near-Term Artificial Gravity Concepts for Deep Space Missions.* Retrieved from NASA Technical Reports Server (NTRS): https://ntrs.nasa.gov/archive/nasa/casi.ntrs.nasa.gov/20190000843.pdf